

Distance Assisted Recursive Testing

Xuechan Li* Anthony D. Sung[†] Jichun Xie [‡]

March 23, 2022

Abstract

In many applications, a large number of features are collected with the goal to identify a few important ones. Sometimes, these features lie in a metric space with a known distance matrix, which partially reflects their co-importance pattern. Proper use of the distance matrix will boost the power of identifying important features. Hence, we develop a new multiple testing framework named the Distance Assisted Recursive Testing (DART). DART has two stages. In stage 1, we transform the distance matrix into an aggregation tree, where each node represents a set of features. In stage 2, based on the aggregation tree, we set up dynamic node hypotheses and perform multiple testing on the tree. All rejections are mapped back to the features. Under mild assumptions, the false discovery proportion of DART converges to the desired level in high probability converging to one. We illustrate by theory and simulations that DART has superior performance under various models compared to the existing methods. We applied DART to a clinical trial in the allogeneic stem cell transplantation study to identify the gut microbiota whose abundance will be impacted by the after-transplant care.

Keywords: Multiple testing, aggregation tree, false discovery proportion (FDP), auxiliary information

*Xuechan Li is a PhD candidate of Biostatistics at Duke University.

[†]Anthony D. Sung is an Assistant Professor of Medicine at Duke University.

[‡]Jichun Xie is an Associate Professor of Biostatistics and Bioinformatics at Duke University.

1 Introduction

A typical multiple testing problem aims to identify a small number of important features among many with a controlled false discovery rate, typically referred to as “finding needles in a haystack”. In many applications, these features lie in a metric space where their pairwise distances are known. For example, in neuro-imaging studies, the distance between two neurons can be calculated based on their 3D location and the brain anatomy structure; in genomic studies, the distance between any two genomic sequences can be calculated based on their nucleotide differences; and in spatial analysis, the Euclidean distances between two sites can be calculated via their geometric locations. In these examples, neurons, genomic sequences, and geometric locations are features of interest. Very often, important features tend to cluster with each other. For example, in genomic studies, two similar genomic sequences often perform similar biological functions. If one plays an important role, then the other is likely to play a similar role. This implies that the distance matrix can be viewed as the auxiliary information – if properly used, it will boost the testing power.

Some existing methods are aware that the feature ordering or distance partially implies their co-importance patterns. One approach is to use the hidden Markov chain (Sun and Cai, 2009) or the hidden Markov random fields (Liu et al., 2012; Shu et al., 2015; Lee and Lee, 2016) to model the latent importance status of features. The co-importance patterns are introduced by the inferred transition probabilities. These approaches have two major limitations. First, to infer the transition probabilities, these methods assume the test statistics follow multivariate Gaussian distributions. This assumption limits the scope of the application. Second, although nice theoretical properties can be derived under the hidden Markov chain model, for complex hidden Markov random fields models, it is challenging to prove the asymptotic validity; to the best of our knowledge, no paper so far has succeeded. Alternatively, Zhang et al. (2011) developed a method called FDR_L . FDR_L pre-specified a smoothing window. For each hypothesis, it smooths the p-value across its local neighbors within the window. However, the window

size is set as a common tuning parameter, which is not fully adaptive to the distance. Recently, Cai et al. (2020) developed a locally-adaptive weighting and screening method named LAWS. LAWS weighted the p-value using the estimated local sparsity level, which is structure-adaptive based on a pre-specified kernel function. However, the performance of LAWS heavily depends on the accuracy in local sparsity level estimation, which in general is difficult. In addition, LAWS focus on a setting that the features are located in a regular lattice and require a non-vanishing proportion of features to be important. These conditions might not hold for many high-dimensional feature selection problems.

In this paper, we propose a new framework of multiple testing that utilizes the distance matrix as auxiliary information to boost testing power, called the Distance Assisted Recursive Testing (DART). It has two stages.

- **Stage I: Transform the distance matrix into a static aggregation tree.** On the bottom layer (layer 1), each leaf is a set containing a feature; on higher layers, leaves are hierarchically aggregated to nodes based on the distance. Thus, a nodes is a set containing one or more features. Figure 1 shows a toy example. Layer 1 has 7 leaves, $A_1^{(1)} = \{1\}, \dots, A_7^{(1)} = \{7\}$; on layer 2, leaves with maximum distance no larger than $g^{(2)} = 2$ are aggregated, resulting in nodes $A_1^{(2)} = \{1, 2\}$, $A_2^{(2)} = \{3, 4, 5\}$, $A_3^{(2)} = \{6\}$, $A_4^{(2)} = \{7\}$; on layer 3, nodes with maximum distance no larger than $g^{(3)} = 5$ are aggregated, resulting in the parent nodes $A_1^{(3)} = A_1^{(2)} \cup A_2^{(2)} = \{1, 2, 3, 4, 5\}$ and $A_2^{(3)} = A_3^{(2)} \cup A_4^{(2)} = \{6, 7\}$.

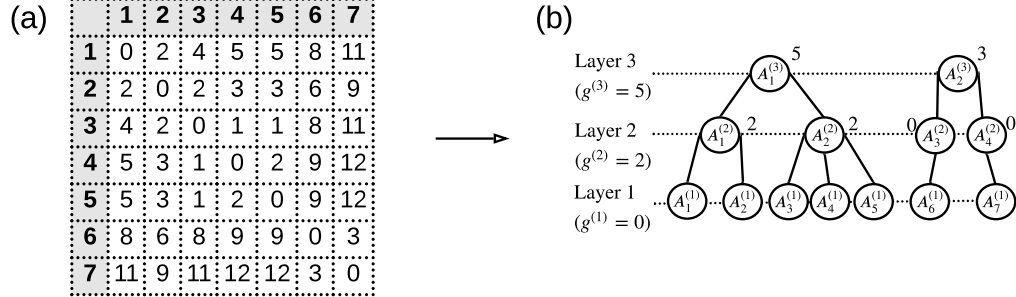
- **Stage II: Set up dynamic node hypotheses and perform multiple testing on the tree.**

The testing procedure is recursive. On each layer, we exclude the rejected features from the static nodes on the tree and turn them into dynamic working nodes. For each working node, we formulate a dynamic node hypothesis to test the collective effect of all features in the node. If we reject a node, all its features will be rejected. The rejected nodes and their corresponding features will be removed from the next layer. This procedure

will continue till the algorithm stops. Figure 1(c) provides an illustration. On layer 1, $S_1^{(1)} = A_1^{(1)} = \{1\}$ and $S_3^{(1)} = A_3^{(1)} = \{3\}$ is rejected and removed from the tree; on layer 2, the dynamic working node $S_2^{(2)} = A_2^{(2)} \setminus \{3\} = \{4, 5\}$ is rejected, and thus features 4 and 5 are rejected; and on layer 3, the dynamic working node $S_2^{(3)} = \{6, 7\}$ is rejected, and thus features 6 and 7 are rejected. A single layer testing procedure will only reject features $\{1, 3\}$, while the 3-layer DART will reject the features $\{1, 3, 4, 5, 6, 7\}$. The multi-layer DART will lead to more discoveries while still asymptotically controlling the feature-level FDR.

Generally speaking, DART is a multiple testing method with a hierarchical structure. Some other multiple testing methods also adopt hierarchical or graphical structures. Goeman and Mansmann (2008) developed a family-wise error rate (FWER) controlling procedure to perform gene ontology (GO) analysis. The procedure split the GO graph into m subgraphs at the focus level. On the subgraph, it tests whether a set of genes are significantly associated with the phenotype and control their FWER. Later, the FWER controlling procedure has been extended to trees and directed acyclic graphs (DAG) (Goeman and Finos, 2012; Meijer and Goeman, 2015). Dmitrienko et al. (2007) and Dmitrienko and Tamhane (2013) developed methods testing hierarchically ordered hypotheses with applications to clinical trials and control FWER. Yekutieli (2008) considers the case when all the original hypotheses represent a node on the tree and develop a method to test those hypotheses simultaneously. In their setting, the P-value of the parent node hypothesis is independent of the child node hypothesis, while under our model the parent node P-values depend on the child node P-values. Guo et al. (2018) developed a per-family error rate (PFER) and FDR controlling procedure for hypotheses with a DAG structure. Soriano and Ma (2017) develops a multiple testing procedure embedded in the partition tree. To identify where two distributions differ, it starts from testing low resolution hypotheses (parent hypotheses) first and automatically split the low resolution hypotheses into high resolution hypotheses (child hypotheses) and control the overall FDR. Li et al. (2020) developed a bottom-up multiple testing approach with some similarities to our testing procedure

Stage I: Transform the distance matrix into a static aggregation tree



Stage II: Set up dynamic node hypotheses and perform multiple testing on the tree

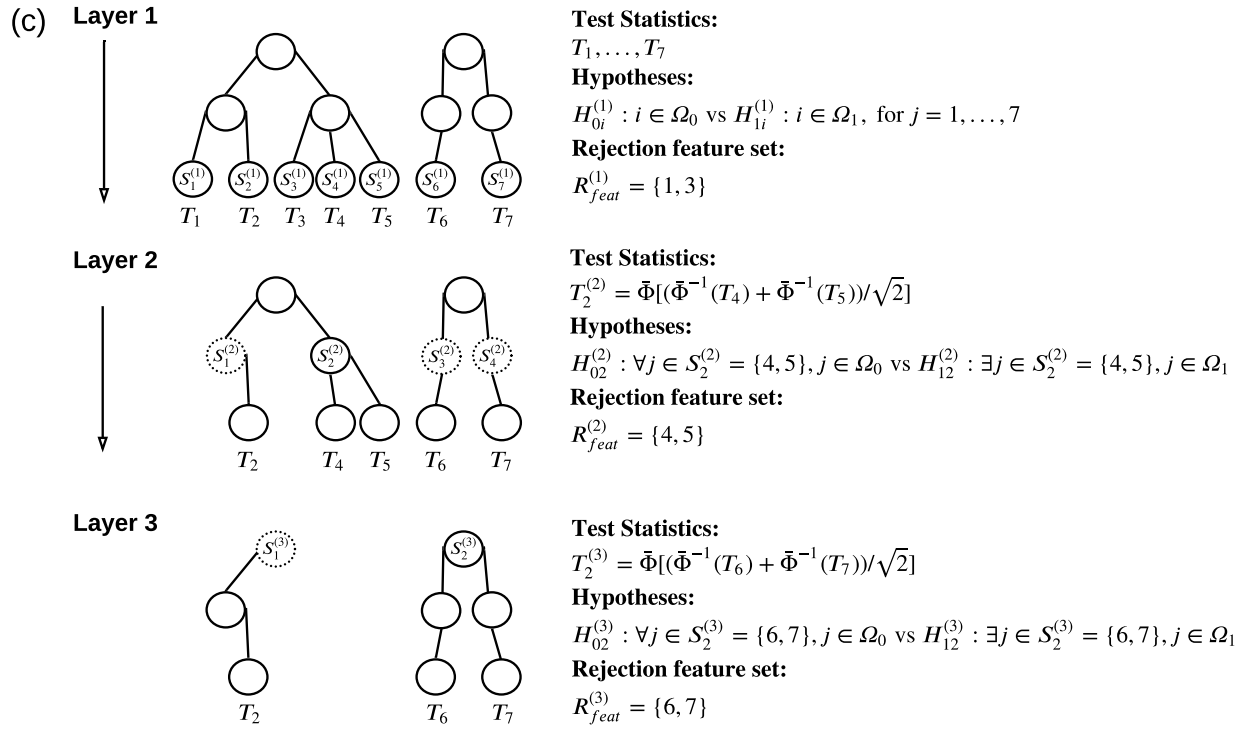


Figure 1: An illustrating example of DART with 7 features. In stage I, we converge the distance matrix in (a) to a 3-layer aggregation tree in (b). In stage II, we perform multiple testing embedded in tree (b). The testing procedures are illustrated in (c).

embedded on the aggregation tree.

Although the existing methods have achieved some success in many application scenarios, they are not directly applicable to our problem due to three reasons. First, in our problem, the hierarchical structure between our features is not intrinsic but has to be constructed via the distance matrix. Second, our method assumes natural dependence between parent and child nodes hypotheses, while most existing methods require independence among all node hypotheses. Third, most existing methods define type I error on all the nodes across all layers. Such type I error measure can hardly be mapped back to feature-level FDR (on the bottom layer) and thus cannot be directly applied to general multiple testing problems. Technically speaking, we innovatively extended the FDR control approaches and asymptotic theories from static hypotheses to dynamic hypotheses, making the general multiple testing framework adaptive to many complicated design.

The rest of the paper is organized as follows. Section 2 describes the general DART algorithm. Section 3 justifies the asymptotic properties of DART under mild conditions. Section 4 shows that under various models, DART has superior performance than the existing methods. Section 5 applies DART to the microbiome data collected from the leukemia patients before and after the hematopoietic cell transplantation. Section 6 provides a brief discussion on the possible extension of DART. More details about the framework and the proofs of main theorems are provided in the Appendix.

2 Method

2.1 Model

Denote by $\Omega = \{1, \dots, m\}$ the set with m features, where Ω_1 is the important (alternative) feature set, Ω_0 is the non-important (null) feature set, and $\Omega_1 \cap \Omega_0 = \emptyset$. For feature i , the

hypothesis is

$$H_{0i} : i \in \Omega_0 \quad \text{versus} \quad H_{1i} : i \in \Omega_1. \quad (1)$$

A distance matrix $\mathbf{D} = (d_{ij})_{m \times m}$ is available, where $d_{ij} = d_{ji}$ is the distance between feature i and feature j . For simplicity, we assume the distance matrix is scaled so that $\max_{i \neq j} d_{ij} = 1$. It is easy to see that $d_{ii} = 0$.

As a typical multiple testing problem, for hypothesis $H_{0,i}$, a statistic X_i^* can be summarized and then transformed to a working P-value T_i .

Definition 1 (Oracle P-value property). We call a statistic \tilde{T}_i an oracle P-value if it satisfies the oracle P-value property:

$$\begin{aligned} P(\tilde{T}_i \leq p) &\leq p & \text{if } i \in \Omega_0, \\ P(\tilde{T}_i > p) &\geq p & \text{if } i \in \Omega_1. \end{aligned} \quad (2)$$

Under the ideal circumstance, T_i satisfies the oracle P-value property. However, under many circumstances, there exists another oracle P-value \tilde{T}_i and the working P-value T_i weakly converges to \tilde{T}_i uniformly except at the tail:

$$\sup_{i \in \Omega_0} \sup_{p \in \mathcal{P}_{i0}} \left| \frac{P(T_i < p)}{P(\tilde{T}_i < p)} - 1 \right| = \delta_{0m} \quad \text{with} \quad \lim_{m \rightarrow \infty} \delta_{0m} = 0, \quad (3)$$

where $\mathcal{P}_{i0} = \left\{ p \in [0, 1] : P(\tilde{T}_i < p) \geq \{m(\log m \log \log m)^{1/2}\}^{-1} \right\}$.

Our model puts a weak condition on the working P-value so that in practice DART can be applied to a wide scope of applications. As an illustration, we discuss the linear model where each feature is an outcome. The goal is to test whether the covariates will impact the feature outcomes. A detailed application example where we use this linear model to perform the microbiome analysis is provided in Section 5.

Example 1 (Linear regression with feature outcomes). Suppose Y_1, \dots, Y_m are m feature outcomes and W_1, \dots, W_{p_0} are p_0 covariates; W_1 can be the intercept term. Under more general

settings, W_j can also be feature specific. For feature i , the model is

$$Y_i = \theta_{1,i}W_1 + \dots + \theta_{p_0,i}W_{p_0} + \epsilon_i, \quad (4)$$

where $\boldsymbol{\theta}_i = (\theta_{1,i}, \dots, \theta_{p_0,i})^T$ is the coefficient vector and ϵ_i is the random error with $\epsilon_i \sim N(0, \sigma^2)$. For feature Y_i , the hypothesis is

$$H_{0i} : \mathbf{q}^T \boldsymbol{\theta}_i = 0 \text{ against } H_{Ai} : \mathbf{q}^T \boldsymbol{\theta}_i \neq 0, \text{ for } i = 1, \dots, m.$$

To test the hypotheses, we collect n random samples. Denote the design matrix $\mathcal{W} = (W_{k,j})_{n \times p_0}$, where $W_{k,j}$ is the j th covariate of sample k . Also denote outcome i observations by $\mathbf{Y}_i = (Y_{k,i})_{n \times 1}$, where $Y_{k,i}$ is the i th feature outcome of sample k . Let $\hat{\boldsymbol{\theta}}_i$ be the least squared estimator of $\boldsymbol{\theta}_i$, the test statistic is

$$X_i^* = \left(\frac{\mathbf{q}^T \hat{\boldsymbol{\theta}}_i}{s \sqrt{\mathbf{q}^T (\mathcal{W}^T \mathcal{W})^{-1} \mathbf{q}}} \right)^2,$$

$$\text{where } s^2 = \frac{1}{n-p_0} \left\| \mathbf{Y}_i - \mathcal{W} \hat{\boldsymbol{\theta}}_i \right\|_2^2.$$

The working P-value of feature i is

$$T_i = 1 - F_0(X_i^*), \quad (5)$$

where F_0 is the CDF of the $\chi^2(1)$ distribution. To construct the oracle P-value, we first construct the oracle statistic

$$X_{o,i} = \left(\frac{\mathbf{q}^T \hat{\boldsymbol{\theta}}_i}{\sigma \sqrt{\mathbf{q}^T (\mathcal{W}^T \mathcal{W})^{-1} \mathbf{q}}} \right)^2$$

involving the unknown parameter σ^2 . $X_{o,i}$ exactly follows $\chi^2(1)$. The oracle P-value is $\tilde{T}_i = 1 - F_0(X_{o,i})$. The following lemma shows that the linear regression is a special example of our model.

Lemma 1. Under the linear regression example, the working P-value T_i and the oracle statistics \tilde{T}_i satisfy (3). Moreover, we have

$$\sup_{i \in \Omega} \sup_{p \in \mathcal{P}_{i0}} \left| \frac{P(T_i < p)}{P(\tilde{T}_i < p)} - 1 \right| \rightarrow 0 \quad (6)$$

2.2 Two stages of DART

2.2.1 Stage I: Transform the distance matrix into an aggregation tree

In Stage I, DART transform the distance matrix into an aggregation tree where the stage II multiple testing procedure will be embedded.

We first introduce the notation of a general aggregation tree. Denote an L -layer aggregation tree by $\mathcal{T}_L = \{\mathcal{A}^{(\ell)} : \ell = 1, \dots, L\}$. Here $\mathcal{A}^{(\ell)}$ is the set of nodes on layer ℓ . Any node $A \in \mathcal{A}^{(\ell)}$ is a set of features on layer ℓ . Let $\mathcal{C}(A)$ denote the child node set. The diameter of node A is defined as

$$\text{dia}(A) = \sup_{(i,j) \in A \times A: i \neq j} d_{ij}.$$

For example, on the tree in Figure 1,

$$\begin{aligned} \mathcal{A}^{(1)} &= \{A_1^{(1)}, \dots, A_7^{(1)}\} = \{\{1\}, \dots, \{7\}\}, \\ \mathcal{A}^{(2)} &= \{A_1^{(2)}, A_2^{(2)}, A_3^{(2)}, A_4^{(2)}\} = \{\{1, 2\}, \{3, 4, 5\}, \{6\}, \{7\}\}, \\ \mathcal{A}^{(3)} &= \{A_1^{(3)}, A_2^{(3)}\} = \{\{1, 2, 3, 4, 5\}, \{6, 7\}\}. \end{aligned}$$

For nodes $A_1^{(3)} = \{1, 2, 3, 4, 5\}$, $\mathcal{C}(A_1^{(3)}) = \{A_1^{(2)}, A_2^{(2)}\} = \{\{1, 2\}, \{3, 4, 5\}\}$. Based on the distance matrix shown in Figure 1a, $\text{dia}(A_1^{(3)}) = 5$.

In stage II, features aggregated into the same node will be tested jointly for their collective effect. To improve the testing performance, a desirable aggregation tree should have the following properties.

- Features should be aggregated based on their distance: two close features should be aggregated before two remote features.
- To increase testing resolution, a desirable tree will have bounded cardinality $|\mathcal{C}(A)| \leq M$, where M is a pre-defined constant.

These two properties inspired us to develop the following algorithm to construct an aggregation tree. On layer 1, each feature forms a leaf, a node (set) containing only the feature index. On layer ℓ with $\ell \geq 2$, each node A is formed by aggregating child nodes on layer $\ell - 1$ with the restriction that

$$\text{dia}(A) \leq g^{(\ell)} \text{ and } |\mathcal{C}(A)| \leq M. \quad (7)$$

We will use the greedy algorithm to construct the tree. See Algorithm 1 for details. Notably, Algorithm 1 is not the only feasible algorithm for aggregation tree construction; yet, the resulting aggregation tree will have the two properties desirable to the stage II testing and thus Algorithm 1 serves the purpose. Also, its computational complexity is $O(m^2 \log m)$, fast enough even for a massive number of features.

2.2.2 Stage II: Set up node hypotheses and perform multiple testing on the tree

Based on the aggregation tree constructed in stage I, the stage II testing procedure is recursive. In other words, on layer ℓ , the working hypotheses and the testing procedure will depend on the testing results on the previous layers.

On layer 1, leaf $\{i\}$ is coupled with the original hypothesis $H_{0,i}$ in (1). We reject $H_{0,i}$ if and only if the working P-value $T_i < \hat{t}^{(1)}$, where $\hat{t}^{(1)}$ is a threshold defined as follows.

$$\hat{t}^{(1)} = \left\{ \alpha_m \leq t \leq \alpha : \frac{mt}{\max\{\sum_{i=1}^m I(T_i < t), 1\}} \leq \alpha, \right\} \quad (8)$$

where $\alpha_m = 1/\{m(\log m)^{1/2}\}$. This testing procedure is similar to the Benjamini and Hochberg procedure (Benjamini and Hochberg, 1995) with minor difference at the tail. Similar procedure

Algorithm 1: Converting the distance matrix to an aggregation tree.

Data: distance matrix $D = (d_{ij})_{m \times m}$, the maximum layer L , the maximum children number M , the maximum aggregatable diameters $g^{(2)}, \dots, g^{(L)}$.

Result: an aggregation tree $\mathcal{T}_L = \{\mathcal{A}^{(\ell)} : \ell = 1, \dots, L\}$ and $\mathcal{C}(A)$ for all $A \in \mathcal{A}^{(\ell)}$ and all $\ell \in \{1, \dots, L\}$.

// initiate the leaves, their children, and the leaf set on layer 1

for $i = 1, \dots, m$ **do**

$A_i^{(1)} = \{i\}; \mathcal{C}(A_i^{(1)}) = \emptyset;$

$\mathcal{A}^{(1)} = \{A_1^{(1)}, \dots, A_m^{(1)}\};$

for $\ell \in \{2, \dots, L\}$ **do**

// on layer ℓ , initiate $\mathcal{A}^{(\ell)}$ and $\tilde{\mathcal{A}}$; $\tilde{\mathcal{A}}$ is a set containing the remaining nodes on layer $\ell - 1$ and the current nodes on layer ℓ

$\tilde{\mathcal{A}} = \mathcal{A}^{(\ell-1)}, \mathcal{A}^{(\ell)} = \emptyset;$

while $|\tilde{\mathcal{A}} \setminus \mathcal{A}^{(\ell)}| > 0$ **do**

// use the greedy algorithm to find the node pair whose diameter is the smallest; if multiple node pairs have a tie, choose any one pair.

$(\check{A}_1, \check{A}_2) = \arg \min_{\{(A_1, A_2) \in \tilde{\mathcal{A}} \times \tilde{\mathcal{A}} : A_1 \neq A_2\}} \text{dia}(A_1 \cup A_2);$

if $\text{dia}(\check{A}_1 \cup \check{A}_2) > g^{(\ell)}$ **then**

// The remaining nodes on layer $\ell - 1$ are too far away so they will stand alone on layer ℓ

for $A \in \tilde{\mathcal{A}} \setminus \mathcal{A}^{(\ell)}$ **do** $\mathcal{C}(A) = A; \mathcal{A}^{(\ell)} = \mathcal{A}^{(\ell)} \cup \{A\}; \tilde{\mathcal{A}} = \emptyset;$

else

// define a new node as the union of two close nodes

$\check{A} = \check{A}_1 \cup \check{A}_2;$

for $i \in \{1, 2\}$ **do**

// check whether \check{A}_i is a current on layer ℓ

if $\check{A}_i \in \mathcal{A}^{(\ell)}$ **then**

$\text{flag}(\check{A}_i) = 1; \mathcal{C}_i = \mathcal{C}(\check{A}_i);$

else

$\text{flag}(\check{A}_i) = 0; \mathcal{C}_i = \{\check{A}_i\};$

$\mathcal{C}(\check{A}) = \mathcal{C}_1 \cup \mathcal{C}_2;$ // for the new node find its child set on layer $\ell - 1$

if $|\mathcal{C}(\check{A})| \leq M$ **then**

// add the new node to layer ℓ and candidate aggregation node on layer $\ell - 1$, and remove its two child nodes

$\mathcal{A}^{(\ell)} = \mathcal{A}^{(\ell)} \cup \{\check{A}\} \setminus \{\check{A}_1, \check{A}_2\}; \tilde{\mathcal{A}} = \tilde{\mathcal{A}} \cup \{\check{A}\} \setminus \{\check{A}_1, \check{A}_2\};$

else

// remove the node on layer ℓ and with larger child node set cardinality

$A^* = \arg \max_{A \in \{\check{A}_1, \check{A}_2\}} \text{flag}(A) \cdot \mathcal{C}(A); \tilde{\mathcal{A}} = \tilde{\mathcal{A}} \setminus \{A^*\};$

have been proposed and discussed in other papers such as Liu et al. (2013) and Xie and Li (2018). After the testing procedure on layer 1, denote the rejected feature set by

$$R_{\text{feat}}^{(1)} = \{i : T_i \leq \hat{t}^{(1)}\}.$$

Unlike other single layer-testing procedure that stops after layer 1, DART will continue testing the accepted hypotheses after aggregating them. Recursively, on layer ℓ ($\ell \geq 2$), suppose the testing on the previous $\ell - 1$ layers yields the rejected feature set

$$R_{\text{feat}}^{1:(\ell-1)} = \bigcup_{\ell'=1}^{\ell-1} R_{\text{feat}}^{(\ell')},$$

where $R_{\text{feat}}^{(\ell')}$ is the rejected feature set on layer ℓ' . Then on layer ℓ , for any node $A \in \mathcal{A}^{(\ell)}$, we define the working node $S(A) = A \setminus R_{\text{feat}}^{1:(\ell-1)}$. The rejected nodes are excluded from $S(A)$ because they have already been rejected and do not need to be tested again. Thus $S(A)$ is dynamic. For example, in Figure 1, node $A_2^{(2)} = \{3, 4, 5\}$ and $S_2^{(2)} = \{4, 5\}$, because feature 3 has been rejected on layer 1.

The child set $\mathcal{C}(S)$ is also dynamic, depending on the rejection path on the previous $\ell - 1$ layers. We denote this rejection path by $\mathcal{Q}^{(1:\ell-1)}$. All possible rejection paths before layer ℓ forms a filtration $\mathfrak{F}^{(1:\ell-1)}$.

Let a

$$\mathcal{B}^{(\ell)} = \{S(A) : A \in \mathcal{A}^{(\ell)}, |\mathcal{C}(S)| \geq 2\}$$

be the working node set. Also let $m^{(\ell)} = \sum_{S \in \mathcal{B}^{(\ell)}} |S|$ be the number of features to be tested on layer ℓ . We exclude the node with only one child because the node must have been tested on some lower layer. For example $S_1^{(2)} = \{2\}$ will not be tested again on layer 2 because it has been tested on layer 1. Notably, although the working nodes on layer ℓ are dynamic, given the rejection path $\mathcal{Q}^{(1:\ell-1)}$, they are determined. For any $S \in \mathcal{B}^{(\ell)}$ ($\ell \geq 2$), we construct the node

hypotheses:

$$H_{0S}^{(\ell)} : \forall j \in S, j \in \Omega_0 \quad \text{versus} \quad H_{1S}^{(\ell)} : \exists j \in S, j \in \Omega_1.$$

To test on layer ℓ , first, we derive the aggregated working P-value for node S by

$$X_j = \bar{\Phi}^{-1}(T_j), \quad X_S = \sum_{j \in S} X_j / \sqrt{|S|}, \quad T_S = \bar{\Phi}(X_S), \quad (9)$$

where $\bar{\Phi}$ is the complementary CDF of the standard Gaussian distribution. Because S is dynamic, the distribution of T_S is meaningful only when all the descendent working nodes of S are accepted. Thus, even if all T_j under the null has independent marginal distribution $\text{Unif}(0, 1)$, T_S might not follow oracle P-value property. Instead, an oracle P-value \tilde{T}_S can be constructed as $\tilde{T}_S = \bar{G}_S(X_S)$, where \bar{G}_S is the conditional complementary CDF of X_S given the rejection path:

$$\bar{G}_S(x) = P(X_S > x \mid \mathcal{Q}^{(1:\ell-1)}).$$

Estimating \bar{G}_S is computationally intensive because all the possible rejection paths need to be considered. For large-scale multiple testing problems, this could be infeasible. To solve this problem, we pretend that X_S follows $N(0, 1)$ and calculate the working P-value T_S as in (9). Although T_S does not condition on the rejection path $\mathcal{Q}^{(1:\ell-1)}$, T_S weakly converges to \tilde{T}_S when \tilde{T}_S is small. In multiple testing, we usually apply small threshold to P-values and thus good approximation to \tilde{T}_S when it is small is sufficiently useful. Later, we will show that this replacement will guarantee the asymptotic validity of DART.

Next on layer ℓ , we define the rejection rule: H_{0S} is rejected if $T_S < \hat{t}^{(\ell)}(\alpha)$. Here

$$\hat{t}^{(\ell)}(\alpha) = \sup \left\{ \alpha_m \leq t \leq \alpha : \frac{\sum_{\ell'=1}^{\ell-1} m^{(\ell')} \hat{t}^{(\ell')} + m^{(\ell)} t}{\max\{\sum_{\ell'=1}^{\ell-1} |R_{\text{feat}}^{(\ell')}| + \sum_{s \in \mathcal{B}^{(\ell)}} |S| I(T_S < t), 1\}} \leq \alpha \right\}, \quad (10)$$

where $\alpha_m = 1/\{m(\log m)\}^{1/2}$. It is easy to see that $\hat{t}^{(\ell)}$ depends on the value of $\hat{t}^{(1)}, \dots, \hat{t}^{(\ell-1)}$. This is natural because the testing procedure is embedded in an aggregation tree and thus

recursive. The denominator of the fraction in (10)

$$\max \left\{ \sum_{\ell'=1}^{\ell-1} |R_{\text{leaf}}^{(\ell')}| + \sum_{S \in \mathcal{B}^{(\ell)}} |S| I(T_S < t), 1 \right\}$$

is the number of the rejected nodes; to take the maximum with 1 is to avoid the denominator to be zero. Intuitively, the numerator

$$\sum_{\ell'=1}^{\ell-1} m^{(\ell')} \hat{t}^{(\ell')} + m^{(\ell)} t \quad (11)$$

$$\lesssim \sum_{\ell'=1}^{\ell-1} \sum_{S \in \mathcal{B}^{(\ell')}} |S| P_{0S}(T_S > \hat{t}^{(\ell')} \mid \mathcal{Q}^{(1:\ell'-1)}) + \sum_{S \in \mathcal{B}^{(\ell)}} |S| P_{0S}(T_S > t \mid \mathcal{Q}^{(1:\ell-1)}) \quad (12)$$

$$\approx \sum_{\ell'=1}^{\ell-1} \sum_{S \in \mathcal{B}^{(\ell')}} |S| I(T_{0S} > \hat{t}^{(\ell')}) I(H_{0S}^{(\ell')} \text{ is true}) + \sum_{S \in \mathcal{B}^{(\ell)}} |S| I(T_{0S} > t) I(H_{0S}^{(\ell)} \text{ is true}) \quad (13)$$

From (11) to (12), we view almost all of the nodes are null nodes and their P-values are asymptotically sub-uniform under the null so that on layer ℓ' , $P_{0S}(T_S > t \mid \mathcal{Q}^{(1:\ell'-1)}) \leq t$. From (12) to (13), we use the empirical average of the indicator functions to approximate the probability. If we assume most nodes either contain all null or all alternative features, then (13) approximates the number of falsely rejected features when using the threshold $(\hat{t}^{(1)}, \dots, \hat{t}^{(\ell-1)}, t)$ on layer 1, \dots , layer $\ell-1$, and layer ℓ .

Finally on layer ℓ , denote the rejected node set on layer ℓ by $\mathcal{R}_{\text{node}}^{(\ell)} = \{S \in \mathcal{B}^{(\ell)} : T_S < \hat{t}^{(\ell)}\}$. Presumably the important features would cluster; thus, for any $S \in \mathcal{R}_{\text{node}}^{(\ell)}$, we will aggressively reject all features in it, $R_{\text{feat}}^{(\ell)} = \bigcup_{S \in \mathcal{R}_{\text{node}}^{(\ell)}} S$.

The testing procedure will continue till layer L , where L is a pre-specified number. Algorithm 2 provides the details of testing on the aggregation tree.

Algorithm 2: Multiple testing on the aggregation tree.

Data: Tree $\mathcal{T}_L = \{\mathcal{A}^{(i)} : i = 1, \dots, L\}$, P-values (T_1, \dots, T_m) , and FDR level α .
Result: The set of rejected features R_{feat} .

// test on layer 1

set $t^{(1)}$ as in (8); $R_{\text{feat}} = \{i : T_i \leq t^{(1)}\}$;

for $\ell \in \{2, \dots, L\}$ **do**

// initiate the node index and P-value vector at the beginning of layer ℓ

$k = 0, T = \text{NULL}$;

for $A \in \mathcal{A}^{(\ell)}$ **do**

$S_k = A \setminus R_{\text{feat}}$;

if $|S_k| \geq 2$ **then**

$k = k + 1; X_{S_k} = \sum_{j \in S_k} \bar{\Phi}^{-1}(T_j) / \sqrt{|S_k|}$;

$T = (T, \bar{\Phi}(X_{S_k}))$;

// append the new node statistic

set $\hat{t}^{(\ell)}(\alpha, T)$ as in (10); $R_{\text{node}}^{(\ell)} = \{S_{k'} : T_{k'} > \hat{t}^{(\ell)}\}$; $R_{\text{feat}} = R_{\text{feat}} \cup \{\cup_{S \in R_{\text{node}}^{(\ell)}} S\}$.

2.3 Tuning parameter selection

The number of total layers L , the maximum cardinality M , and the distance upper bounds $g^{(2)}, \dots, g^{(L)}$ are viewed as tuning parameters. Among many, we list a feasible approach to select the tuning parameters.

1. The maximum cardinality M will affect the testing resolution. If M is too large, then when a large node is rejected, all its contained leaves will be rejected. Under most circumstances, we recommend $M = 3$.
2. We set c_m to a constant (e.g., 30), and hope the number of working nodes on the highest layer exceed this number. On layer L , the number of nodes will be lower bounded by m/M^L . Thus we can select $L = \lceil \log_M m - \log_M c_m \rceil$.
3. Let $g^{(1)} = 0$. Assume $g^{(1)}, \dots, g^{(\ell-1)}$ are set. On layer ℓ , consider a set of values $G^{(\ell)} = \{g_1, \dots, g_K\}$. For any $g \in G^{(\ell)}$, let $\mathcal{A}^{(\ell)}(g)$ be the set of nodes on layer ℓ by setting g as the maximum acceptable diameter. Let $\tilde{\mathcal{A}}^{(\ell)}(g)$ be the set of its non-single-child nodes,

$$\tilde{\mathcal{A}}^{(\ell)}(g) = \{A : A \in \mathcal{A}^{(\ell)}(g), |\mathcal{C}(A)| \geq 2\}. \quad (14)$$

Then we choose $g^{(\ell)}$ as the one that yields the most nodes in $\tilde{\mathcal{A}}^{(\ell)}(g)$,

$$g^{(\ell)} = \arg \max_{g \in G} |\tilde{\mathcal{A}}^{(\ell)}(g)|.$$

The values in $G^{(\ell)}$ can be customized according to the application context; nevertheless, they are meaningful within the range $G_*^{(\ell)} = (0, (2M^{\ell-2} - 1)d_{\max}]$, with

$$d_{\max} = \max_{j \in \{1, \dots, m\}} \min_{i \in \{i: i \neq j\}} d_{ij}.$$

More details about how we choose $g^{(\ell)}$ is shown in Algorithm 3 in Appendix A.

On layer $\ell - 1$, a node would have at most $M^{\ell-2}$ many features. By the triangle inequality in metric space, the distance between a node and its closest neighbor will not exceed $(2M^{\ell-2} - 1)d_{\max}$. This means, on layer ℓ with $g^{(\ell)} = (2M^{\ell-2} - 1)d_{\max}$, any child node on layer $\ell - 1$ will be combined with its closest neighbor if the closest neighbor is not combined with other child nodes. Thus, we let the right-bound of $G_*^{(\ell)}$ be $(2M^{\ell-2} - 1)d_{\max}$.

We will choose $g^{(\ell)}$ such that on layer ℓ there are enough nodes to be potentially tested. Proposition 1 show that with proper maximum aggregatable diameters, $\tilde{\mathcal{A}}^{(\ell)}(g^{(\ell)}) = \Theta(m)$ for $\ell \in \{1, \dots, L\}$ when the distance is embedded in the Euclidean distance. Hereafter, we write $a_m = \Theta(b_m)$ if $b_m = O(a_m)$ and $a_m = O(b_m)$.

Proposition 1. *Consider a d -dimensional space with the Euclidean distance. For any aggregation tree constructed by Algorithm 1 with the finite L and M , we have,*

$$|\tilde{\mathcal{A}}^{(\ell)}(g^{(\ell)})| = \Theta(m).$$

In section 3, we show that any finite integer values of L and M , and any $\{g^{(2)}, \dots, g^{(L)}\}$ with $\tilde{\mathcal{A}}^{(\ell)}(g^{(\ell)}) = \Theta(m)$ leads to asymptotic control on FDR. In the supplementary materials S2, we extend this result to $M = \infty$ numerically.

3 Asymptotic Theory

3.1 Asymptotic Type I error control

In multiple testing, type I error is commonly measured by the false discovery proportion (FDP) and its expectation called the false discovery rate (FDR). Under our model, the FDP and FDR are defined as follows.

$$\text{FDP} = \frac{|R_{\text{feat}}^{(1:L)} \cap \Omega_0|}{|R_{\text{feat}}^{(1:L)}| \vee 1}, \quad \text{FDR} = E(\text{FDP}).$$

Because DART is a recursive testing procedure embedded in the aggregation tree, on layer ℓ , we also define the layer-specific node FDP $^{(\ell)}$ and FDR $^{(\ell)}$ as follows.

$$\text{FDP}^{(\ell)} = \frac{|\mathcal{R}_{\text{node}}^{(\ell)} \cap \mathcal{B}_0^{(\ell)}|}{|\mathcal{R}_{\text{node}}^{(\ell)}| \vee 1}, \quad \text{FDR}^{(\ell)} = E(\text{FDP}^{(\ell)}),$$

where $\mathcal{B}_0^{(\ell)} = \{S \in \mathcal{B}^{(\ell)} : \forall j \in S, j \in \Omega_0\}$ is the set of all null dynamic working nodes. Clearly, FDP $^{(\ell)}$ and FDR $^{(\ell)}$ depend on the filtration $\mathfrak{F}^{(1:\ell-1)}$.

The definition of the overall FDP and FDR is on the feature level, while the definition of layer-specific FDP $^{(\ell)}$ and FDR $^{(\ell)}$ is on the node level. For FDP $^{(\ell)}$ and FDR $^{(\ell)}$, the null nodes are those without any alternative features. There could be some nodes where contain both null and alternative features. When these mixed nodes are rejected, on the node level, they are counted as the true rejections, while on the feature level, the null features in the mixed nodes are falsely rejected. This suggests that controlling the feature-level FDP or FDR is more challenging than controlling the node-level FDP $^{(\ell)}$ and FDR $^{(\ell)}$.

Later in this section, we will show that DART guarantees its FDP bounded by α with a high probability converging to 1. This immediately leads to the asymptotic control of FDR. Theorem 1 shows that the layer specific FDP $^{(\ell)}$ is bounded with a high probability, and Theorem 2 shows the overall FDP is also bounded with a high probability; the latter requires an additional

condition (Condition 4).

Here we list all the conditions.

Condition 1 (Sparse alternatives). Assume $m_1 \leq r_2 m^{r_1}$ for some $r_1 < \frac{1}{M^{L-1}+1}$ and $r_2 > 0$. In addition, there exists a constant $r_3 > 0$, such that $n \geq m^{r_3}$.

Remark 1. Condition 1 assumes the important features are sparse. It also assumes that the total number of features cannot exceed the polynomial order of the sample size. Under this condition, $\hat{t}^{(\ell)}$ is upper bounded by Cm^{r_1-1} with a high probability (Lemma 4).

Condition 2 (Sparse dependent signals). There exists a set of features Γ with $|\Gamma| = o(\frac{\log m}{\log \log m})$, such that $\{T_i : i \in \Omega \setminus \Gamma\}$ are mutually independent.

Very often, when a feature has a strong signal, its working P-value is small. Thus, for any S with $|S| \geq 2$, we define the moderate P-value interval.

$$\kappa(|S|) = \left(m^{-\frac{1-r_1}{|S|-1}}, \{m(\log m \log \log m)^{1/2}\}^{-\frac{1}{|S|}} \right).$$

When $|S| = 1$, we let the left side of $\kappa(|S|)$ be 0. On lower layers, $|S|$ is smaller, and thus both sides of $\kappa(|S|)$ are closer to zero. In addition, as m goes to infinity, both sides of $\kappa(|S|)$ converge to zero and the left side converges faster. In that case, although $\kappa(|S|)$ has a vanishing Lebesgue measure, the alternative working node P-values could also converge to zero and thus the probability $P[T_j \in \kappa(|S|)]$ could be non-vanishing.

Condition 3 (Sufficient moderate signal nodes). On layer ℓ with $1 \leq \ell \leq L$, define

$$\mathcal{G}^{(\ell)} = \{S \in \mathcal{A}^{(\ell)} : |\mathcal{C}(S)| \neq 1, \forall j \in S, P[T_j \in \kappa(|S|)] \geq C\}.$$

Then there exist some constants $r_4 > 0, C \in (0, 1)$ such that

$$|\mathcal{G}^{(\ell)}| \geq r_4 \log m. \quad (15)$$

Remark 2. Later, we will prove that when $S \in \mathcal{G}^{(\ell)}$, the probability of rejection any descendant nodes of S before layer ℓ is negligible, while the probability of rejecting S on layer ℓ is non-negligible.

Remark 3. Condition 3 guarantees that with a high probability, at least $C \log m$ number of hypotheses will be rejected on layer ℓ . This level of expected number of rejections on layer ℓ will avoid leading to a overly small threshold $\hat{t}^{(\ell)}$ in (10); if $\hat{t}^{(\ell)}$ is too small, at the tail, the working P-values may fail to approximate the oracle P-values well and result in an inflation in the type I error.

Remark 4. Condition 3 is technical. If we specify a larger lower bound on $\hat{t}^{(\ell)}$ and do not reject anything when $\hat{t}^{(\ell)}$ satisfying (10) cannot be found, Condition 3 can be removed. However, this might result in a loss in power.

Remark 5. Condition 3 is pretty weak because we only require $C \log m$ nodes on layer ℓ to satisfy the signal strength condition. This order is very small compared to the total number of alternative nodes on layer ℓ , which could reach Cm^{r_1} .

Let $\Omega_{st}^{(1:0)} = \emptyset$, define the strong signal node set on each layer recursively as

$$\begin{aligned}\mathcal{G}_{st}^{(\ell)} &= \{S \in \mathcal{A}^{*,(\ell)} : \forall j \in S, P(T_j \in \kappa(|S|)) > 1 - o(m^{-r_1})\}, \\ \Omega_{st}^{(1:\ell)} &= \left\{ \cup_{S \in \mathcal{G}_{st}^{(\ell)}} S \right\} \cup \Omega_{st}^{(1:\ell-1)}.\end{aligned}$$

Here,

$$\mathcal{A}^{*,(\ell)} = \{A \setminus \Omega_{st}^{(1:\ell-1)} : A \in \mathcal{A}^{(\ell)}\}.$$

Based on the definition, $\Omega_{st}^{(1:L)}$ is set of the features with strong signals in all of the layers. Later, we will prove that with a high probability converging to 1, none of the features in $\cup_{S \in \mathcal{G}_{st}^{(\ell)}} S$ will be rejected from layer 1 to layer $\ell - 1$ but all of them will be rejected on layer ℓ .

Define the weak signal P-value interval and the weak signal set

$$\iota = (0, m^{r_1-1}], \quad \Omega_{\text{wk}} = \{j \in \Omega_1 : P(T_j \in \iota) = O(m^{r_1-1})\}.$$

When a node S contains only null features and weak signal features, then the probability of rejecting S is negligible.

Definition 2 (mixed nodes). For any set S , let

$$S^* = S \setminus (\Omega_{\text{st}}^{(1:L)} \cup \Omega_{\text{wk}}), \quad S_0^* = S^* \cap \Omega_0, \quad S_1^* = S^* \cap \Omega_1. \quad (16)$$

If $S_0^* \neq \emptyset$ and $S_1^* \neq \emptyset$, we call S a mixed node.

Condition 4 (Sparse mixed nodes). Let $\mathcal{P} = \{S \in \mathcal{A}^{(L)} : S \text{ is a mixed node}\}$. Then $|\mathcal{P}| = o(\log m)$.

Remark 6. Condition 4 assumes that the mixed nodes on layer L (the highest layer) are very rare. Equivalently, this means the dominating majority of the nodes contain: 1) only null features; 2) only alternative features; 3) a combination of null and alternative features but all alternative features are either weak- or strong-signal features. Because the aggregation tree is constructed based on the distance matrix, this condition can be translated as how distance informs hypothesis states (null or alternative). To prove the consistence of the overall FDP, we need this condition because our rejection rule aggressively rejects all features in a node if the node is rejected. Without Condition 4 we might reject too many mixed nodes so that the type I error on the feature level will be inflated.

Remark 7. The constraints $|\mathcal{P}| = o(\log m)$ can be relaxed to $|\mathcal{P}| = o(\mathcal{G}^{(\ell)})$. The number of mixed nodes need to be of a smaller order of the number of moderate signal nodes on the same layer.

Theorem 1 (Layer-specific node $\text{FDR}^{(\ell)}$ control). *Under Conditions 1-3, at any pre-specified level $\alpha \in (0, 1)$, DART satisfies the following two statements.*

(1) For any $\epsilon > 0$, $\lim_{m,n \rightarrow \infty} P(FDP^{(\ell)} \leq \alpha + \epsilon) = 1$. Consequently, $\lim_{m,n \rightarrow \infty} FDR^{(\ell)} \leq \alpha$.

(2) Let $\tilde{\Omega}_0 = \{j : \tilde{T}_j \text{ follows } \text{Unif}(0, 1)\}$, where \tilde{T}_j is the oracle P-value of feature j . If

$$\lim_{m \rightarrow \infty} |\tilde{\Omega}_0|/m = 1, \quad (17)$$

then for all $\epsilon > 0$,

$$\lim_{m,n \rightarrow \infty} P(|FDP^{(\ell)} - \alpha| \leq \epsilon) = 1, \quad \lim_{m,n \rightarrow \infty} FDR^{(\ell)} = \alpha.$$

The strategies to prove (1) and (2) in Theorem 1 are similar. Here, we briefly discuss the sketch of the proof of (1). The main step is to show that

$$P \left\{ \frac{1}{\sum_{S \in \mathcal{B}_0^{(\ell)}} |S|} \sum_{S \in \mathcal{B}_0^{(\ell)}} |S| I(T_S < \hat{t}^{(\ell)}) \leq t^{(\ell)} \right\} \rightarrow 1, \quad \text{as } m, n \rightarrow \infty. \quad (18)$$

Notably, $\hat{t}^{(\ell)} \in [\alpha_m, \alpha]$ based on (10). However, within this range, (18) might not hold. We used Conditions 1 and 3 to further narrow the range of $\hat{t}^{(\ell)}$ with a high probability converging to 1. We prove that $\hat{t}^{(\ell)} \in [\Theta(\log m/m), \alpha]$ with a high probability converging to 1. Within this new range, (18) holds.

Theorem 2 (Overall feature FDR control). *Under Conditions 1-4, at any pre-specified level $\alpha \in (0, 1)$, DART satisfies the following two statements.*

(1) For any $\epsilon > 0$, $\lim_{m,n \rightarrow \infty} P(FDP \leq \alpha + \epsilon) = 1$. Consequently, $\lim_{m,n \rightarrow \infty} FDR \leq \alpha$.

(2) If (17) holds, then for any $\epsilon > 0$,

$$\lim_{m,n \rightarrow \infty} P(|FDP - \alpha| \leq \epsilon) = 1, \quad \lim_{m,n \rightarrow \infty} FDR = \alpha.$$

3.2 Conditions on signal strength for linear regressions

We discussed the weak, moderate, and strong signals with respect to the working P-value probabilistic ranges. Under concrete parametric models, these probabilistic ranges can be transformed to more concrete signal strength conditions, which are easier to understand and interpret. Here we consider the linear regression with feature outcomes discussed in Example 1. We specify what ranges of the coefficient signals are considered as weak, moderate, or strong signals. Recall that in Example 1, the oracle P-value is calculated based on the oracle statistic

$$X_{o,i} = \left(\frac{\mathbf{q}^T \hat{\boldsymbol{\theta}}_i}{\sigma \sqrt{\mathbf{q}^T (\mathbf{W}^T \mathbf{W})^{-1} \mathbf{q}}} \right)^2.$$

Let

$$\hat{\tau}_i = \frac{\mathbf{q}^T \hat{\boldsymbol{\theta}}_i}{\sigma \sqrt{\mathbf{q}^T (\mathbf{W}^T \mathbf{W})^{-1} \mathbf{q}}}, \quad \text{and} \quad \tau_i = \frac{\mathbf{q}^T \boldsymbol{\theta}_i}{\sigma \sqrt{\mathbf{q}^T (\mathbf{W}^T \mathbf{W})^{-1} \mathbf{q}}}.$$

Clearly, $X_{o,i} = \hat{\tau}_i^2$ and $E(\hat{\tau}_i) = \tau_i$. Thus, τ_i can be viewed as the signal level of feature i .

Proposition 2. Define

$$\beta = \sqrt{2(1 - r_1) \log m - 2 \log \log m}, \quad \gamma = \sqrt{2 \log m + \frac{1}{2} \log \log \log m}, \quad \lambda = \sqrt{2r_1 \log m}.$$

When $|S| = 1$, define $\frac{\beta}{\sqrt{(|S|-1)}} = +\infty$. Then under linear model in Example 1, the corresponding $\mathcal{G}^{(\ell)}$, $\mathcal{G}_{st}^{(\ell)}$, and Ω_{wk} in Condition 3 and Condition 4 can be defined as

$$\begin{aligned} \mathcal{G}^{(\ell)} &= \left\{ S \in \mathcal{A}^{(\ell)} : \forall j \in S, \frac{\gamma}{\sqrt{|S|}} < |\tau_j| < \frac{\beta}{\sqrt{(|S|-1)}} \right\}, \\ \mathcal{G}_{st}^{(\ell)} &= \left\{ S \in \mathcal{A}^{*,(\ell)} : \forall j \in S, \frac{\gamma}{\sqrt{|S|}} + \lambda < |\tau_j| < \frac{\beta}{\sqrt{(|S|-1)}} - \lambda \right\}, \\ \Omega_{wk} &= \left\{ j \in \Omega_1 : |\tau_j| = o(1/\sqrt{\log m}) \right\}. \end{aligned}$$

Remark 8. Based on condition 1, we have $r_1 < \frac{1}{M^{L-1} + 1}$. Thus, $\frac{\beta}{\sqrt{|S|-1}} > \lambda$ for all $S \in \mathcal{A}^{*,(\ell)}$. However, it is possible that $\frac{\gamma}{\sqrt{|S|}} + \lambda > \frac{\beta}{\sqrt{(|S|-1)}} - \lambda$ for a S with large cardinality. If it happens,

the S does not belong to $\mathcal{G}_{\text{st}}^{(\ell)}$. Thus, $\mathcal{G}_{\text{st}}^{(\ell)}$ could be empty on higher layers as $|S|$ becomes larger. Given the $\mathcal{G}_{\text{st}}^{(\ell)}$ is a set of strong signals that could be exempted from the co-importance pattern reflected by the distance matrix, whether it is empty does not impact the asymptotic performance of DART.

4 Numerical results

In this section, the simulation results are carried out to evaluate the performance of DART. We simulate m features located in the two-dimensional Euclidean space with randomly generated location coordinates: the first coordinate follows $N(0, 2)$, and the second coordinate follows $\text{Unif}(0, 4)$. A distance matrix $\mathbf{D} = (d_{i,j})_{m \times m}$ is calculated based on the feature location coordinates. Two different feature settings are considered, $m = 100$ and $m = 1000$. When $m = 100$, we generate $m_1 = 22$ alternative, and $n = 90$ samples. When $m = 1000$, we generate $m_1 = 141$ alternatives, and $n = 300$ samples.

Based on the tuning parameter selection criterion in Section 2.3, we construct a 2-layer aggregation tree when $m = 100$ and a 4-layers aggregation tree when $m = 1000$. More details about the tuning parameters settings and their selection procedure are shown in appendix A.

We consider five different model settings, SE1–SE5. SE1 simulates the working P-values satisfying the oracle P-value property, and thus mimics the ideal situation. SE2 and SE3 simulates the working P-values by mis-specifying the null distributions, and thus these P-values do not satisfy the oracle P-value property. We use these two settings to evaluate the robustness of DART and the competing methods. SE4 simulates the linear regression model and SE5 simulates the Cox proportional hazard model. We are interested to see how DART compares to the competing methods under these two commonly used models. In each setting, the simulation is repeated 200 times. The R code for running DART is available at https://github.com/xxli8080/DART_Code.

Before we display the five settings, we first introduce the following notations that are used across all five settings:

F_0 : the CDF of $\mathcal{X}^2(1)$ distribution;

$$\eta_{1,i} = \{[2\phi_1(d_{22,i}) - 0.2] \vee 0\} + \{\phi_2(d_{7,i})\};$$

$$\eta_{2,i} = \{[3.4\phi_3(d_{156,i}) - 0.8] \vee 0\} + 3\{\phi_4(d_{7,i})\}$$

$$+ 10 * I(i \in \{100, 200, 300, 400, 500, 600, 700, 800, 900, 1000\}),$$

where ϕ_1, ϕ_2, ϕ_3 and ϕ_4 are the PDF of $N(0, 1)$, $N(0, 0.1)$, $N(0, 0.8)$ and $N(0, 0.05)$, respectively.

SE1: For node $i \in \{1, \dots, m\}$, the feature P-value $T_i = 1 - F_0(\check{Z}_i^2)$, where the $\check{Z}_1, \dots, \check{Z}_m$ are independently generated from $N(\sqrt{n}\theta_i, 1)$, with

$$\theta_i = \begin{cases} \frac{2}{5}\eta_{1,i}I(\eta_{1,i} - 0.15 > 0), & (n, m) = (90, 100) \\ \frac{1}{7}\eta_{2,i}I(\eta_{2,i} - 0.15 > 0), & (n, m) = (300, 1000). \end{cases}$$

SE2: For node $i \in \{1, \dots, m\}$, the feature P-value $T_i = 1 - F_0(\check{Z}_i^2)$, where the $\check{Z}_1, \dots, \check{Z}_m$ are independently generated from $\text{Laplace}(\sqrt{n}\theta_i, 1)$, with

$$\theta_i = \begin{cases} \frac{3}{5}\eta_{1,i}I(\eta_{1,i} - 0.15 > 0), & (n, m) = (90, 100) \\ \frac{1}{6}\eta_{2,i}I(\eta_{2,i} - 0.15 > 0), & (n, m) = (300, 1000) \end{cases}$$

SE3: For node $i \in \{1, \dots, m\}$, the feature P-value $T_i = 1 - F_0(\check{Z}_i^2)$, where the $\check{Z}_1, \dots, \check{Z}_m$ are independently generated from the non-central student t distribution with 2 degree of freedom and none centrality parameter $\sqrt{n}\theta_i$, with

$$\theta_i = \begin{cases} \frac{1}{6}\eta_{1,i}I(\eta_{1,i} - 0.15 > 0), & (n, m) = (90, 100) \\ \frac{1}{14}\eta_{2,i}I(\eta_{2,i} - 0.15 > 0), & (n, m) = (300, 1000) \end{cases}$$

SE4: Consider the linear mode defined in (4), with $p_0 = 3$, and $\sigma = 1$. In model (4), $W_1 = 1$ is the intercept term, W_2 and W_3 are sampled from $\text{Binom}(0.5)$ and $\text{Unif}(0.1, 0.5)$, respectively. Also let $\theta_{1,i} = \theta_{3,i} = 0.1$ and

$$\theta_i = \theta_{1,i} = \begin{cases} 2\eta_{1,i}I(\eta_{1,i} - 0.15 > 0), & (n, m) = (90, 100) \\ \frac{5}{6}\eta_{2,i}I(\eta_{2,i} - 0.15 > 0), & (n, m) = (300, 1000) \end{cases}$$

The feature P-value T_i is defined in (5).

SE5: Consider the cox regression model

$$\lambda_i(t) = \lambda_{0i}(t) \exp\{\theta_{1,i}W_1 + \theta_{2,i}W_2\}$$

Where $\lambda_i(t)$ and $\lambda_{0i}(t)$ is the hazard and baseline hazard at time t , respectively. Set $\theta_{0,i} = \theta_{2,i} = 0.1$ and

$$\theta_i = \theta_{1,i} = \begin{cases} \frac{4}{5}\eta_{1,i}I(\eta_{1,i} - 0.15 > 0), & (n, m) = (90, 100) \\ \frac{2}{7}\eta_{2,i}I(\eta_{2,i} - 0.15 > 0), & (n, m) = (300, 1000) \end{cases}$$

The covariates W_1 and W_2 are sampled from $\text{Binom}(0.5)$ and $\text{Unif}(0.1, 0.5)$, respectively. The event time is generated from the exponential distribution with rate $\exp\{\theta_{1,i}W_1 + \theta_{2,i}W_2\}$, and the censoring time is sampled from $\text{Unif}(0, 5)$. The feature P-value T_i is obtained from the Wald test.

Throughout the five settings, the hypotheses are:

$$H_{0,i} : \theta_i = 0 \quad \text{against} \quad H_{1,i} : \theta_i \neq 0, \quad i \in \Omega.$$

We set the nominal FDR at the level $\alpha = 0.05, 0.1, 0.15, 0.20$. DART successfully controlled the empirical FDR under the desired level. The FDR control is robust when the model is

misspecified. Figure 2 shows how DART performs when the algorithm stopped at different layers. Obviously, the one-layer DART is the same as the traditional single layer multiple testing method which ignores the distance matrix. As the number of maximum layers L goes up, more clustered alternative features are aggregated and identified. Notably, increasing the nominal FDR level cannot lead to such great increase in sensitivity.

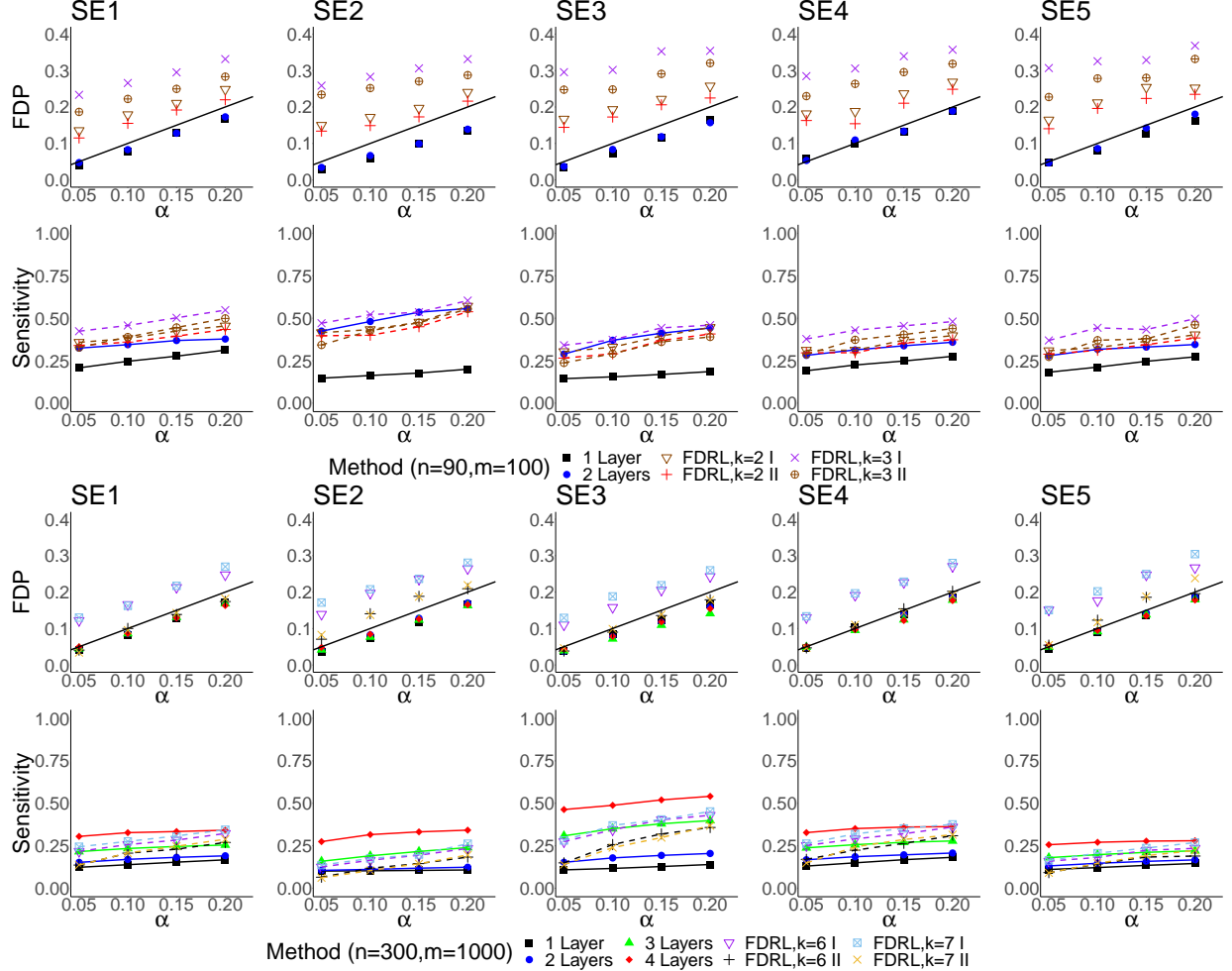


Figure 2: Simulation results for setting SE1-SE5. The first two rows represent the results in the setting $(n, m) = (90, 100)$, and the second two rows represent the results in the setting $(n, m) = (300, 1000)$.

We also compared the performance of DART with the two FDR_L procedures (FDR_L I and FDR_L II) proposed by Zhang et al. (2011). The two procedure adjust each feature's P-value according to its k -nearest neighbors; the adjusted p-value is the median of its neighborhood p-values. The FDR_L I and FDR_L II procedures use different methods to estimate the distribution

of the adjusted P-values. We compared to both procedures in our simulation. To be objective, we also tried a wide range of choices $k \in \{2, 3, \dots, 9\}$. When $(n, m) = (90, 100)$, both FDR_L I and FDR_L II led to inflations in FDR no matter what k we used. When $(n, m) = (300, 1000)$, the FDR_L I procedure constantly led to inflated FDR, while the FDR_L II procedure led to the desired FDR when $k \leq 7$ but the sensitivity is lower than DART. Figure 2 presents the performance of FDR_L procedures with $k = 2, 3$ when $(n, m) = (90, 100)$ and $k = 6, 7$ when $(n, m) = (300, 1000)$, because under these k settings, the FDR_L procedures perform the best.

One main reason that the FDR_L procedures did not perform as well as DART is that the methods use a constant k to aggregate P-values. Very often, the distance among features often cannot be fully captured by the neighborhood with constant number of neighbors. For example, an feature far away from all other features also have k nearest neighbors; however, the isolated feature and its neighbors often do not share co-importance. Thus, FDR_L does not perform well under these settings.

5 Data Analysis

We apply DART to a clinical trial on the hematopoietic stem cell transplantation (HCT), where microbiome data are collected from each leukemia patient before and after the HCT. Graft-versus-host disease (GVHD) is one of the major complications of the HCT. Recent studies have linked GVHD to the disruptions of the gut microbiome (Jenq et al., 2012), and the disruptions may be related to the environmental changes such as after-transplant care (Claesson et al., 2012). Based on those findings, the analysis objective is to investigate the potential impact of the after-transplantation care (home care versus standard hospital care) on the microbiome composition. The patient fecal samples are collected before and after HCT; the fecal microbiome are sequenced by the 16S ribosomal RNA sequencing at the Memorial Sloan Kettering Cancer Center. The data are then pre-processed by the R package, DADA2 (Callahan et al., 2016), to generate the amplicon sequence variants (ASV) and the read counts. Samples with

less than 200 total read counts and the ASVs with read counts fewer than 4 in more than 80% of the samples are removed from the analysis. After the pre-processing procedure, the data set contains 288 samples (before- and after- HCT) from 144 patients, each with 97 ASVs. The data are available at https://github.com/xxli8080/DART_Code/tree/master/Data_Analysis. In our analysis, to increase computation stability, the zero counts are replaced by 0.5. This replacement is commonly used in the microbiome data analysis (Aitchison, 1982; Kurtz et al., 2015).

In microbiome studies, the ASV abundance compositions are more meaningful than the absolute read counts. To modeling the compositional microbiome data, we use the additive log-ratio (alr) transformation proposed by Aitchison (1982). Specifically, we choose the most abundant ASV (the ASV with the largest median read counts across all patients) as the reference ASV, and define M_i as the log read counts ratio between the ASV i and the reference ASV. For example, for a patient, if the read counts of ASV i and the reference ASV are 100 and 200 respectively, then $M_i = \log(100/200) = -\log 2$.

Because one ASV is chosen as the reference ASV, the distance matrix is calculated among the remaining 96 non-reference ASV using the R package `Phangorn` (Schliep, 2011) based on the JC69 model (Jukes et al., 1969). The JC69 model is a classical Markov model of DNA sequence evolution and can be used to estimate the evolutionary distance between sequences. Two ASVs with similar sequences tend to be close with each other, and more likely to perform similar biological functions. Therefore, we will incorporate the distance matrix in identifying the important ASVs. We use the linear model, defined in (4) with $p_0 = 3$, to regress the microbiome composition changes before and after HCT on the after-transplantation care (home care vs. hospital care) and other covariates. Specifically, for the non-reference ASV i , $i \in \{1, \dots, 96\}$,

$$M_{1,i} - M_{0,i} = \theta_{1,i}W_1 + \theta_{2,i}W_2 + \theta_{3,i}W_3 + \epsilon_i \quad (19)$$

Here, $M_{0,i}$ (and $M_{1,i}$) is the log counts ratio between ASV i and the reference ASV before (and

after) the transplant. Thus $M_{1,i} - M_{0,i}$ is the corresponding Y_i in (4). In addition, $W_1 = 1$ is the intercept term, W_2 is the type of care, W_3 is the length of the care (the gap between the HCT surgery and the after-care sample collection), and the $\epsilon \sim N(0, \sigma^2)$ is the random error term with unknown σ^2 . To check whether the after-transplant care affects the ASV compositions, we set up the hypotheses $H_{0i} : \theta_{2,i} = 0, i = 1, \dots, 96$. The P-value T_i are calculated based on the Wald test.

Based on the tuning parameter selection procedure described in Section 2.3, we construct an aggregation tree with $M = 3$, $L = \lceil \log_M 96 - \log_M 30 \rceil = 2$, and $g^{(2)} = \frac{8}{\sqrt{144 \log 96 \log \log 96}}$. The aggregation tree has 33 non-single-child nodes on the second layer. The nominal FDR level is set at 0.1.

The performance of the DART is compared with two competing methods: 1) BH procedure; 2) FDR_L . For the FDR_L I and II procedures, we considered $k = 2$ or 3. Figure 3(a) shows that the ASVs that are close to each other tend to have similar (small or large) P-values. This suggests that the co-importance pattern among similar ASVs might hold here. In the end, the two-layer DART identified 9 important ASVs while the traditional BH procedure did not identify any ASV. Both FDR_L I and FDR_L II procedures identified 14 important ASVs when $k = 2$. When $k = 3$, FDR_L I identified 16 important ASVs, and FDR_L II identified 7 important ASVs.

In order to evaluate the stability of these methods, we conduct the bootstrap with 200 resamplings. For a specific testing method, the rejection rate of an ASV is calculated as the ratio of the times that the ASV is identified in the 200 rounds of resamplings. If a method is stable, an ASV should tend to be consistently rejected or accepted. In other words, for a valid and powerful test, most null ASVs are expected to have small rejection rates, and very few alternative ASVs are expected to have high rejection rates. Figure 3(b) shows that DART and BH procedures generates the histograms with a peak rejection rate between 0 – 0.2, while FDR_L have the peak rejection rate between 0.1 – 0.3. Table 1 listed the proportion of ASVs with large (> 0.8) or small (≤ 0.1) rejection rates for each method. Compared with FDR_L method, DART and BH have a higher proportion of ASVs with small rejection rates, indicating

both DART and BH have lower risk in FDR inflation. DART also has a higher proportion of ASVs with large rejection rates comparing to the BH method, slightly lower but same order of large rejection rates as FDR_L procedures. This indicates that DART has a robust high power.

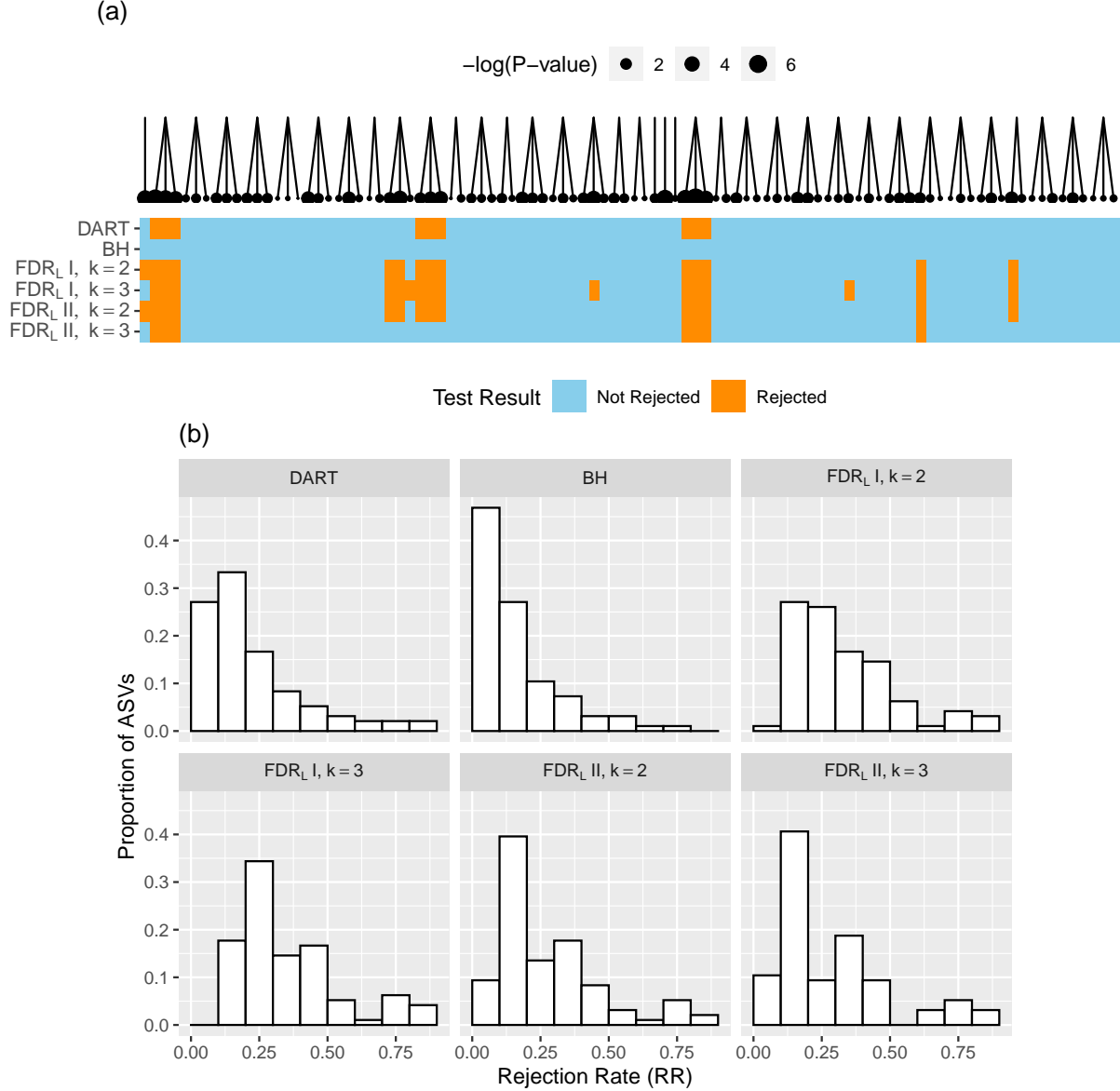


Figure 3: (a) Illustration of the leaf P-values, the aggregation tree, and the testing results. The leaf size is scaled according to the inverse of the P-values. The testing results of different methods are shown in different rows, with blue blocks representing the accepted non-reference ASVs and orange blocks representing the rejected non-reference ASVs. (b) Histograms of ASV rejection rate across the bootstrap with 200 re-samplings.

Table 1: Summary of the bootstrap results. (RR stands for rejection rates)

Method	RR ≤ 0.1	RR > 0.8
DART	0.27	0.02
BH	0.47	0
FDR_L I, $k = 2$	0.01	0.03
FDR_L I, $k = 3$	0	0.04
FDR_L II, $k = 2$	0.09	0.02
FDR_L II, $k = 3$	0.1	0.03

6 Discussion

In this paper, we developed a novel multiple testing method, DART, that incorporates the feature distance to hierarchically test a large number of hypotheses. In many application contexts, the distance among features serve as auxiliary information of their co-importance pattern. DART utilizes this information to boost the testing power. DART applies to general working P-values, and thus can work with a wide range of models.

Stage 1 of DART involves constructing an aggregation tree. We provided Algorithm 1 to construct the aggregation tree. Other algorithms may also work, and result in a different aggregation tree from the same distance matrix. Consequently, Stage 2 testing process could lead to different results based on different trees. In practice, if several aggregation trees exist, DART can be applied to all of them, and we can take the one with the most rejections. The asymptotic validity will still hold for this procedure.

DART is a multiple testing method embedded in a hierarchical tree that constructed from the distance matrix. It can be easily extended to the case where other information implies the co-importance pattern of the features. Such information could come from domain knowledge, external data sets, or other resources. In addition, the hierarchical testing ideas and techniques can also be extended to solve other multiple testing problems.

Appendix

The appendix includes 2 sections. Section A provides specific algorithm for choosing tuning parameter and additional numerical results. Section B provides the proof of main theorems.

A Tuning Parameter Selection

The section 2.3 introduces the tuning parameter selection for the aggregation tree construction. Based on it, the tuning parameter for our numerical study is selected as follow:

- If $(n, m) = (90, 100)$: Based on recommendation in section 2.3, we choose $M = 3$ and construct a $L = \lceil \log_M 100 - \log_M 30 \rceil = 2$ layers aggregation tree.

We use Algorithm 3 to construct a dynamic set G and search the value $g^{(2)}$. Table 2 (1) tracks the number of non-single-child nodes $|\tilde{A}^{(2)}(g)|$ based on different values of $g \in G$. By applying the algorithm,

$$g^{(2)} = 26 / \sqrt{n \log m \log \log m}$$

- If $(n, m) = (300, 1000)$: Similar to the previous case, we choose $M = 3$ and construct a $L = \lceil \log_M 1000 - \log_M 30 \rceil = 4$ layers aggregation tree. Based on Algorithm 3, we have Table 2 which tracks the number of non-single-child nodes on each layer, and,

$$g^{(2)} = \frac{8}{\sqrt{n \log m \log \log m}}$$
$$g^{(3)} = \frac{22}{\sqrt{n \log m \log \log m}}$$
$$g^{(4)} = \frac{56}{\sqrt{n \log m \log \log m}}$$

Algorithm 3: $g^{(\ell)}$ Selection algorithm.

Data: Distance Matrix $D = (d_{ij})_{m \times m}$, Sample size n , number of features m , the maximum children number M , the maximum layer L

Result: $g^{(2)}, \dots, g^{(L)}$.

// set searching upper bound d_{\max} and step-size $s_{n,m}$

Let $d_{\max} = \max_{j \in \Omega} \min_{i \in \{i: i \neq j\}} d_{ij}$; $s_{n,m} = 2/\sqrt{n \log(m) \log \log(m)}$;

for $\ell = 2, \dots, L$ **do**

// on layer ℓ , search $g^{(\ell)}$ from $(g^{(\ell-1)}, d_{\max}]$, $g^{(1)} = 0$

Let $M_g = \text{NULL}$; $m_g = 0$; $G = \text{NULL}$; $g = g^{(\ell-1)} + s_{n,m}$;

while $g \leq (2M^{L-2} - 1)d_{\max}$ **do**

// stop searching process if the value g exceed the searching upper bound.

Use Algorithm 1 to Construct an ℓ layers aggregation tree

$\mathcal{T}_\ell = \{\mathcal{A}^{(\ell')} : \ell' = 1, \dots, \ell\}$ with maximum children number M , and

$(g^{(1)}, \dots, g^{(\ell-1)}, g)$;

Set $\tilde{A}^{(\ell)}(g)$ as in (14);

$G = (G, g)$; $M_g = (M_g, |\tilde{A}^{(\ell)}(g)|)$; $m_g = |\tilde{A}^{(\ell)}(g)|$;

$g = g + s_{n,m}$;

$g^{(\ell)} = \min\{\arg \max_{g \in G} M_g\}$;

Table 2: The number of non-single-child nodes based on value $g \in G$ when $M = 3$. For simplisity purpose, the value g is represented by its nominator: $g' = g \times \sqrt{n \log m \log \log m}$. The selected g' and its correspnding $|\tilde{A}^{(2)}(g)|$ is highlighted in bold.

(1) $(n, m) = (90, 100)$:

Layer 2	g'	2	4	6	8	10	12	14	16	18	20	22	24	26	28	30	32	...
	$ \tilde{A}^{(3)}(g) $	5	10	17	22	29	31	31	39	40	40	40	40	41	41	41	41	...

(2) $(n, m) = (300, 1000)$:

Layer 2	g'	2	4	6	8	10	12	14	16	...							
	$ \tilde{A}^{(2)}(g) $	49	149	245	293	293	293	293	293	...							
Layer 3	g'	10	12	14	16	18	20	22	24	26	28	30	...				
	$ \tilde{A}^{(3)}(g) $	103	154	191	221	230	239	241	241	241	241	241	...				
Layer 4	g'	...	38	40	42	44	46	48	50	52	54	56	58	60	62	64	...
	$ \tilde{A}^{(4)}(g) $...	116	118	119	120	120	120	120	120	120	121	121	121	121	121	...

B Proof of the Main Theorems

Before the proof, we need to introduce some further notations. On layer ℓ , for a working node $S \in \mathcal{B}^{(\ell)}$, let $\mathcal{U}(S) = \{S' \subset S : S' \in \cup_{\ell'=1}^{\ell-1} \mathcal{B}^{(\ell')}\}$ be the collection of sets in the testing path of S . In addition, let $\mathcal{U}^c(S) = \{S'' \in \cup_{\ell'=1}^{\ell-1} \mathcal{B}^{(\ell')} : S'' \subset \cup_{A \in \mathcal{A}^{(\ell)}} A \setminus S\}$ be the collection of sets that are planned to be combined with S on layer ℓ of the static aggregation tree but rejected on previous layers. When $S \in \mathcal{B}^{(1)}$, we set $\mathcal{U}(S) = \mathcal{U}^c(S) = \emptyset$. We define $G_S(c)$ as the complementary CDF conditional on previous testing results. When $\ell = 1$, we have $S = \{i\} \subset \{1, \dots, m\}$, and $G_S(c) = P(Z_i \geq c)$ with $Z_1, \dots, Z_m \stackrel{iid}{\sim} N(0, 1)$. When $\ell > 1$, the oracle rejection path for set $S \in \mathcal{B}^{(\ell)}$ is recursively defined as

$$\mathcal{Q}_z^{(1:\ell-1)} = \{z : \forall S' \in \mathcal{U}(S), G_{S'}(Z_{S'}) \geq \hat{t}^{(\ell_{S'})}(\alpha), \forall S'' \in \mathcal{U}^c(S), G_{S''}(Z_{S''}) \leq \hat{t}^{(\ell_{S''})}(\alpha)\},$$

and

$$G_S(c) = P(Z_S \geq c | \mathcal{Q}_z^{(1:\ell-1)})$$

Here, $Z_S = \sum_{i \in S} Z_i / \sqrt{|S|}$, and $\ell_{S'}, \ell_{S''} \in \{1, \dots, \ell - 1\}$ is the value s.t. $S' \in \mathcal{B}^{(\ell_{S'})}$ and $S'' \in \mathcal{B}^{(\ell_{S''})}$, respectively.

Based on condition 2, majority of the signals are mutually independent. Thus, for majority of the set $S \in \mathcal{B}^{(\ell)}$,

$$G_S(c) = P(Z_S \geq c | \forall S' \in \mathcal{U}(S), G_{S'}(Z_{S'}) \geq \hat{t}^{(\ell_{S'})}(\alpha))$$

Given the definition of $G_S(c)$, we define the rejection path as

$$\mathcal{Q}^{(1:\ell-1)} = \{x : \forall S' \in \mathcal{U}(S), G_{S'}(X_{S'}) \geq \hat{t}^{(\ell_{S'})}(\alpha), \forall S'' \in \mathcal{U}^c(S), G_{S''}(X_{S''}) \leq \hat{t}^{(\ell_{S''})}(\alpha)\} \quad (20)$$

In addition, for two sequences of real numbers a_m and b_m , we write $a_m = o(b_m)$ when $\frac{a_m}{b_m} \rightarrow 0$, and $a_m = O(b_m)$ when $\lim_{m \rightarrow \infty} |a_m/b_m| \leq C$ for some constant C . To prove the asymptotic

properties of DART, we need the following lemmas.

Lemma 2. Let $\mathcal{P}_i = \{p \in [0, 1] : P(\tilde{T}_i < p) \geq \epsilon(m)\}$ and $\mathcal{P}'_i = \{p \in [0, 1] : P(\tilde{T}_i < p) \geq \epsilon(m)\epsilon'(m)\}$, with $\epsilon(m), \epsilon'(m) \rightarrow 0$. For any set of independent random variable $\hat{T}_i \in [0, 1]$, and a collection $\mathcal{M} = \{S \subset \{1, \dots, m\} : |S| < c_0\}$ with some constant c_0 ,

$$(1) \text{ If } \max_{i \in \mathcal{M}} \sup_{p \in \mathcal{P}'_i} \left| \frac{P(\hat{T}_i < p)}{P(\tilde{T}_i < p)} - 1 \right| \rightarrow 0, \text{ then,}$$

$$\sup_{S_0 \in \mathcal{M}} \sup_{p \geq \epsilon(m)} \left| \frac{P(\sum_{i \in S_0} \hat{X}_i > c_{S_0}(p))}{P(\sum_{i \in S_0} \tilde{X}_i > c_{S_0}(p))} - 1 \right| \rightarrow 0,$$

$$(2) \text{ If } \lim_{m \rightarrow \infty} \max_{i \in \{1, \dots, m\}} \sup_{p \in \mathcal{P}'_i} \left(\frac{P(\hat{T}_i < p)}{P(\tilde{T}_i < p)} - 1 \right) \leq 0, \text{ then,}$$

$$\lim_{m \rightarrow \infty} \sup_{S_0 \in \mathcal{M}} \sup_{p \geq \epsilon(m)} \left(\frac{P(\sum_{i \in S_0} \hat{X}_i > c_{S_0}(p))}{P(\sum_{i \in S_0} \tilde{X}_i > c_{S_0}(p))} - 1 \right) \leq 0$$

Here, $\hat{X}_i := \bar{\Phi}^{-1}(\hat{T}_i)$, $\tilde{X}_i := \bar{\Phi}^{-1}(\tilde{T}_i)$ and $c_{S_0}(p)$ is the value s.t. $P[\sum_{i \in S_0} \tilde{X}_i > c_{S_0}(p)] = p$.

Lemma 3. Let $\mathcal{B}_{01}^{(\ell)} = \{S \in \mathcal{B}_0^{(\ell)} : S \cap \Gamma = \emptyset\}$, we have

$$\max_{\ell \in \{2, \dots, L\}} \max_{S \in \mathcal{B}_{01}^{(\ell)}} \sup_{c \in [\beta, \gamma]} \left| \frac{G_S(c)}{\bar{\Phi}(c)} - 1 \right| \rightarrow 0$$

Lemma 4. Define

$$\mathcal{X}^{(\ell)} = \left\{ x : \sum_{S \in \mathcal{B}_0^{(\ell)}} |S| I(T_S < \hat{t}^{(\ell)}) - \sum_{S \in \mathcal{B}_0^{(\ell)}} |S| \hat{t}^{(\ell)} \leq \left\{ \sum_{S \in \mathcal{B}_0^{(\ell)}} |S| \hat{t}^{(\ell)} \right\} \epsilon \right\} \quad (21)$$

Then, $\forall \ell = 1, \dots, L$, when the FDR control holds on layer $1, \dots, \ell - 1$,

(1) For all $\epsilon \in (0, \alpha)$, if $P(m\hat{t}^{(\ell)} \geq c \log m) \rightarrow 1$, then $P(\mathcal{X}^{(\ell)}) = 1 - o(1)$.

(2) On $\cap_{h=1}^{\ell} \mathcal{X}^{(h)}$, there exist a constant C s.t.

$$\hat{t}^{(\ell)} \leq Cm^{r_1-1}.$$

(3) Let \hat{c}_S be the rejection threshold for the test node $S \in \mathcal{B}^{(\ell)}$, s.t. $\bar{G}_S(\hat{c}_S) = \hat{t}^{(\ell)}$. Then on

$$\cap_{h=1}^{\ell} \mathcal{X}^{(h)},$$

$$\hat{c}_S > \beta, \forall S \in \mathcal{B}^{(\ell)},$$

and on $\cap_{h=1}^{\ell-1} \mathcal{X}^{(h)}$,

$$\hat{c}_S < \gamma, \forall S \in \mathcal{B}^{(\ell)}.$$

Lemma 5.

$$\frac{\sum_{S \in \mathcal{B}_0^{(\ell)}} |S| \hat{t}^{(\ell)}}{\sum_{S \in \mathcal{B}^{(\ell)}} |S| I(T_S < \hat{t}^{(\ell)})} = \alpha(1 + o(1)) \quad (22)$$

Proof of Proposition 1. Let $\mathcal{A}_s^{(\ell)} := \{S \in \mathcal{A}^{(\ell)} : |\mathcal{C}(S)| = 1\}$ be the set of single-child node on layer ℓ . If $|\mathcal{A}_s^{(\ell)}| = o(m)$, then it is trivial that $\tilde{\mathcal{A}}^{(\ell)} = \Theta(m)$. So it is suffice to show that when $|\mathcal{A}_s^{(\ell)}| = \Theta(m)$, we have $|\tilde{\mathcal{A}}^{(\ell)}| = \Theta(m)$.

Given the $g^{(\ell)}$ is selected from the interval $G_*^{(\ell)}$ as the one that yields the most nodes in $\tilde{\mathcal{A}}^{(\ell)}(g)$.

It is suffice to show that $\tilde{\mathcal{A}}^{(\ell)}(g) = \Theta(m)$ when $g = (2M^{\ell-2} - 1)d_{\max}$. Since

- On layer $\ell \geq 2$, the nearest neighbor of a single-child node is grouped with other nodes.
- For a non-single child node $S' \in \mathcal{A}^{(\ell)}$, define $\mathcal{N}(S') = \{S \in \mathcal{A}_s^{(\ell)} : \text{dia}(S \cup S') < g\}$. Then in the d-dimensional Euclidean space, the $|\mathcal{N}(S')|$ is upper bounded by a constant C .

We have $|\tilde{\mathcal{A}}^{(\ell)}(g)| = \Theta(m)$. □

Proof of Proposition 2.

(1)

For $\ell = 1, \dots, L$, $\forall j \in S \in \mathcal{G}^{(\ell)}$, since $|\eta_j| \in \left(\frac{\gamma+\lambda}{\sqrt{|S|}}, \frac{\beta-\lambda}{\sqrt{|S|-1}}\right)$, we have

$$P\left[\tilde{T}_j \in \kappa(|S|)\right] \geq P\left[\frac{\beta}{\sqrt{(|S|-1)}} \geq \tilde{X}_j \geq \frac{\gamma}{\sqrt{|S|}}\right] \rightarrow 1$$

Based on the asymptotic properties of the student's t-distribution, we have $P(T_j \in \kappa(|S|)) \geq C$.

(2)

For any $S \in \mathcal{G}_{\text{st}}^{(\ell)}$,

$$\begin{aligned} P(\tilde{T}_i > m^{-\frac{1-r_1}{|S|-1}}) &\geq P\left(|\tilde{X}_i| < \sqrt{\frac{2(1-r_1)}{|S|-1} \log m - 2 \log \log m}\right) \\ &\geq P\left(|\tilde{X}_i| < \frac{\beta}{|S|-1} (1 - 1/\sqrt{\log m})\right) \\ &= 1 - o(m^{-r_1}) \end{aligned}$$

Similarly, we have $P(\tilde{T}_i > \{m(\log m \log \log m)^{1/2}\}^{-\frac{1}{|S|}}) \geq 1 - o(m^{-r_1})$. Thus, $P(\tilde{T}_j \in \kappa(|S|)) > 1 - o(m^{-r_1})$ and accordingly $P(T_j \in \kappa(|S|)) > 1 - o(m^{-r_1})$.

(3)

When $|\eta_j| = o(1/\sqrt{\log m})$, we have

$$P(\tilde{T}_j < m^{r_1-1}) = 2\bar{\Phi}\left(\sqrt{2(1-r_1) \log m - \log \log m} + o(1/\sqrt{\log m})\right) = O(m^{r_1-1})$$

Based on the asymptotic properties of the student's t-distribution, we have $P(T_j < m^{r_1-1}) = O(m^{r_1-1})$.

Thus, based on (1)-(3), the $\mathcal{G}^{(\ell)}$, $\mathcal{G}_{\text{st}}^{(\ell)}$ and Ω_{wk} can be parametrically defined in the form of proposition 2.

□

Proof of Theorem 1. Since the proof of the theorem statement (2) is similar to the proof of the theorem statement (1), we will only focusing on the proof of statement (1).

The random variable $FDP^{(\ell)}$ can be decomposed to the product of two parts.

$$FDP^{(\ell)} = \frac{\sum_{S \in \mathcal{B}_0^{(\ell)}} |S| I\{T_S < \hat{t}^{(\ell)}\}}{\sum_{S \in \mathcal{B}_0^{(\ell)}} |S| \hat{t}^{(\ell)}} \times \frac{\sum_{S \in \mathcal{B}_0^{(\ell)}} |S| \hat{t}^{(\ell)}}{\max(\sum_{S \in \mathcal{B}^{(\ell)}} |S| I\{T_S < \hat{t}^{(\ell)}\}, 1)} \quad (23)$$

Based on (23), in order to prove

$$\lim_{m \rightarrow \infty} P(FDP^{(\ell)} \leq \alpha + \epsilon) = 1, \quad (24)$$

for all $\epsilon > 0$, we only need prove

$$\lim_{m \rightarrow \infty} P \left\{ \frac{\sum_{S \in \mathcal{B}_0^{(\ell)}} |S| I\{T_S < \hat{t}^{(\ell)}\}}{\sum_{S \in \mathcal{B}_0^{(\ell)}} |S| \hat{t}^{(\ell)}} - 1 < \epsilon \right\} \rightarrow 1 \quad (25)$$

$$\lim_{m \rightarrow \infty} P \left\{ \left| \frac{\sum_{S \in \mathcal{B}_0^{(\ell)}} |S| \hat{t}^{(\ell)}}{\max(\sum_{S \in \mathcal{B}^{(\ell)}} |S| I\{T_S < \hat{t}^{(\ell)}\}, 1)} - \alpha \right| > \epsilon \right\} \rightarrow 0 \quad (26)$$

(26) is immediately followed by Lemma 5, and we will prove (25) by induction. Below is a list of the proof sketch:

1. On layer 1, show $P(m\hat{t}^{(1)} \geq c \log m) \rightarrow 1$. Then, by applying Lemma 4, we have
 - $P(\mathcal{X}^{(1)}) \rightarrow 1$, which is equivalent to (25). Hence, we proved the FDR control on layer 1.
 - $P(\beta < \hat{c}_S < \gamma, \forall S \in \mathcal{B}^{(1)}) \rightarrow 1$, and $P(\hat{c}_S < \gamma, \forall S \in \mathcal{B}^{(2)}) \rightarrow 1$. Note that although this conclusion is not used to prove the FDR control on the current layer, but is necessary to guarantee the FDR control on higher layers.
2. On layer $\ell \geq 2$, assume the FDR control holds on previous layers and $P(\mathcal{X}^{(\ell')}) \rightarrow 1$ for all $\ell' = 1, \dots, \ell - 1$. Then by Lemma 4, $P(\beta < \hat{c}_S < \gamma, \forall S \in \cup_{\ell'=1}^{\ell-1} \mathcal{B}^{(\ell')}) \rightarrow 1$, and

$P(\hat{c}_S < \gamma, \forall S \in \mathcal{B}^{(\ell)}) \rightarrow 1$. Accordingly, we can get $P(m\hat{t}^{(1)} \geq c \log m) \rightarrow 1$. Then, by applying the Lemma 4 again, we have

- $P(\mathcal{X}^{(\ell)}) \rightarrow 1$, which is equivalent to (25). Hence, we proved the FDR control on layer ℓ .
- $P(\beta < \hat{c}_S < \gamma, \forall S \in \mathcal{B}^{(\ell)}) \rightarrow 1$, and $P(\hat{c}_S < \gamma, \forall S \in \mathcal{B}^{(\ell+1)}) \rightarrow 1$.

We start the proof on layer 1.

Layer 1:

The proving for (25) on layer 1 includes two steps: (i) $m\hat{t}^{(1)} \geq c \log m$ with probability 1; (ii) Get (25) by (i).

(i)

Take a subset $\mathcal{F}^{(1)} \subset \mathcal{G}^{(1)}$, such that $|\mathcal{F}^{(1)}| = r_4 \log m$. For any $i \in \mathcal{F}^{(1)}$, we have

$$P(X_i > \gamma) \geq (1 - \delta_1(m))(1 - \delta_3(m)) \rightarrow 1$$

Thus,

$$\sum_{i \in \mathcal{F}^{(1)} \setminus \Gamma} P(X_i > \gamma) \geq r_4 \log m + o(1) \quad (27)$$

By Hoeffding's inequality, we have:

$$P \left(\left| \sum_{i \in \mathcal{F}^{(1)} \setminus \Gamma} I(X_i > \gamma) - \sum_{i \in \mathcal{F}^{(1)} \setminus \Gamma} P(X_i > \gamma) \right| \geq \sqrt{r_4 \log m \log \log m} \right) \leq (\log m)^{-2}$$

Combined with (27), we have

$$\begin{aligned}
& \mathbb{P} \left[\sum_{1 \leq i \leq m} I(T_i \leq \hat{t}^{(1)}) \geq r_4 \log m (1 + o(1)) - 2\sqrt{\log m \log \log m} \right] \\
& \geq \mathbb{P} \left[\sum_{i \in \mathcal{F}^{(1)} \setminus \Gamma} I(X_i > \gamma) \geq r_4 \log m (1 + o(1)) - 2\sqrt{\log m \log \log m} \right] \\
& \geq 1 - o(1)
\end{aligned}$$

Therefore, by Lemma 5, we have

$$\mathbb{P} [m_0 \hat{t}^{(1)} \geq C^{(1)} \log m] \geq 1 - o(1) \quad (28)$$

(ii)

By Lemma 4 (1), $\mathbb{P}(\mathcal{X}^{(1)}) \rightarrow 1$, and accordingly, $\mathbb{P}(FDP^{(1)} < \alpha + \epsilon) \rightarrow 1$.

Layer ℓ :

Based on similar arguments on Layer 1, it is suffice to show

$$\mathbb{P}(m_0 \hat{t}^{(\ell)} > c \log m) \rightarrow 1.$$

Assume $\forall h = 1, \dots, \ell - 1$, $\mathbb{P}(\mathcal{X}^{(h)}) \rightarrow 1$, then by Lemma 4, we have $\mathbb{P}(\beta < \hat{c}_S < \gamma, \forall S \in \mathcal{B}^{(h)}) \rightarrow 1$, and $\mathbb{P}(c_S < \gamma, \forall S \in \mathcal{B}^{(\ell)}) \rightarrow 1$

Let $\mathcal{F}^{(\ell)} \subset \mathcal{G}^{(\ell)}$ with $|\mathcal{F}^{(\ell)}| = \frac{r_4}{2} \log m$ and $\cup_{S \in \mathcal{F}^{(\ell)}} S \subset \Omega \setminus \Gamma$, define

$$\hat{\mathcal{F}}^{(\ell)} = \left\{ S \in \mathcal{B}^{(\ell)} \cap \mathcal{F}^{(\ell)} : T_S < \frac{1}{m\sqrt{\log m}} \right\}$$

By condition 3, there exists some constant c_1 s.t.

$$\begin{aligned} \mathbb{P}(S \in \hat{\mathcal{F}}^{(\ell)}) &= \mathbb{P}(T_S < \frac{1}{m\sqrt{\log m}}, S \in \mathcal{B}^{(\ell)} \cap \mathcal{F}^{(\ell)}) \geq \mathbb{P}\left(\gamma/|S| < X_j < \beta/(|S| - 1), \forall j \in S\right) \\ &\geq c_1 \end{aligned} \tag{29}$$

By Chebyshev's inequality,

$$\begin{aligned} \mathbb{P}\left\{\left|\hat{\mathcal{F}}^{(\ell)}\right| - \sum_{S \in \mathcal{F}^{(\ell)}} \mathbb{P}(S \in \hat{\mathcal{F}}^{(\ell)})\right\} &> \left\{\sum_{S \in \mathcal{F}^{(\ell)}} \mathbb{P}(S \in \hat{\mathcal{F}}^{(\ell)})\right\}^{1/2} (\log m)^{1/4} \\ &\leq \frac{\sum_{S \in \mathcal{F}^{(\ell)}} \mathbb{P}(S \in \hat{\mathcal{F}}^{(\ell)})\{1 - \mathbb{P}(S \in \hat{\mathcal{F}}^{(\ell)})\}}{(\log m)^{1/2} \sum_{S \in \mathcal{F}^{(\ell)}} \mathbb{P}(S \in \hat{\mathcal{F}}^{(\ell)})} = (\log m)^{-1/2} \end{aligned} \tag{30}$$

Define

$$\hat{\mathcal{X}}^{(\ell)} = \{|\hat{\mathcal{F}}^{(\ell)}| \geq c(\log m)\}$$

Then by equation (30), $\mathbb{P}(\hat{\mathcal{X}}^{(\ell)}) \geq 1 - o(1)$.

On $\hat{\mathcal{X}}^{(\ell)}$, we have

$$\sum_{S \in \mathcal{B}_1^{(\ell)}} I(T_S \leq \hat{t}^{(\ell)}) \geq c \log m$$

Then, by applying the similar arguments in the proof of layer 1, based on Hoeffding's inequality and Lemma 3, we can conclude that

$$\mathbb{P}(m_0 \hat{t}^{(\ell)} \geq C^{(\ell)} \log m) \geq 1 - o(1)$$

for some constant $C^{(\ell)}$. □

Proof of Theorem 2. Let $\mathcal{V}^{(\ell)} = \{S \in \mathcal{B}_0^{(\ell)} : S \subset \mathcal{R}^{(\ell)}\}$ and $\mathcal{W}^{(\ell)} = \{S \in \mathcal{B}_1^{(\ell)} : S \subset \mathcal{R}^{(\ell)}\}$ be

the false rejection node set and the rejection node set on layer ℓ , respectively. Define

$$\mathcal{X}_1 = \{S \in \cup_{\ell=2}^L \mathcal{W}^{(\ell)} : S \cap \Omega_{\text{st}}^{(1:L)} \neq \emptyset \text{ and } S \cap \Omega_0 \neq \emptyset\}$$

$$\mathcal{X}_2 = \{S \in \cup_{\ell=2}^L \mathcal{W}^{(\ell)} : S \cap \Omega_{\text{wk}} \neq \emptyset, S \setminus (\Omega_0 \cup \Omega_{\text{wk}}) = \emptyset \text{ and } S \cap \Omega_0 \neq \emptyset\}$$

$$\mathcal{X}_3 = \{S \in \cup_{\ell=2}^L \mathcal{W}^{(\ell)} : S \cap \Omega_1 \setminus (\Omega_{\text{wk}} \cup \Omega_{\text{st}}^{(1:L)}) \neq \emptyset \text{ and } S \cap \Omega_0 \neq \emptyset\}$$

Then,

$$P(\mathcal{X}_1 \neq \emptyset) \leq P(\mathcal{X}_1 \neq \emptyset | \mathcal{X}) P(\cap_{\ell=1}^L \mathcal{X}^{(\ell)}) + P((\cap_{\ell=1}^L \mathcal{X}^{(\ell)})^c) \leq Cm^{r_1} o(m^{-r_1}) + o(1) \rightarrow 0$$

$$P(\mathcal{X}_2 \neq \emptyset) \leq P(\mathcal{X}_2 \neq \emptyset | \mathcal{X}) P(\mathcal{X}) + P(\mathcal{X}^c)$$

$$\stackrel{(a)}{\leq} Cm^{r_1} P \left[X_S \geq \beta \middle| S \in \Omega_{\text{wk}} \cup \Omega_0, \mathcal{X} \right] P(\mathcal{X}) + o(1)$$

$$\stackrel{(b)}{\leq} Cm^{r_1} P \left[X_S \geq \beta \middle| S \in \Omega_{\text{wk}} \cup \Omega_0 \right] + o(1)$$

$$\stackrel{(c)}{\leq} Cm^{r_1} O(m^{r_1-1}) + o(1)$$

$$\rightarrow 0$$

Here, the inequality (a) and (b) is based on Lemma 4 (3) and (1), respectively. The inequality (c) follows Lemma 2. Accordingly,

$$\begin{aligned}
\text{P}(\text{FDP} > \alpha + \epsilon) &\leq \text{P}(\mathcal{X}_1 \cup \mathcal{X}_2 \neq \emptyset) + \text{P}\left(\frac{\sum_{\ell=1}^L \sum_{S \in \mathcal{V}^{(\ell)}} |S|}{\sum_{\ell=1}^L \sum_{S \in \mathcal{R}_{\text{node}}^{(\ell)}} |S|} > \alpha + \epsilon, \mathcal{X}_1 \cup \mathcal{X}_2 = \emptyset\right) \\
&\leq o(1) + \text{P}\left(\frac{\sum_{\ell=1}^L \sum_{S \in \mathcal{V}^{(\ell)} \setminus \mathcal{X}_3} |S| + \sum_{S \in \mathcal{X}_3} |S|}{\sum_{\ell=1}^L \sum_{S \in \mathcal{R}_{\text{node}}^{(\ell)}} |S|} > \alpha + \epsilon\right) \\
&\leq o(1) + \text{P}\left(\frac{\sum_{\ell=1}^L \sum_{S \in \mathcal{V}^{(\ell)} \setminus \mathcal{X}_3} |S| + |\mathcal{P}|}{\sum_{\ell=1}^L \sum_{S \in \mathcal{R}_{\text{node}}^{(\ell)}} |S|} > \alpha + \epsilon\right) \\
&\leq o(1) + \text{P}\left(\sup_{\ell=1}^L \frac{\sum_{S \in \mathcal{V}^{(\ell)} \setminus \mathcal{X}_3} |S|}{\sum_{S \in \mathcal{R}_{\text{node}}^{(\ell)}} |S|} > \alpha + \epsilon + o(1)\right) \\
&\leq o(1) + \sum_{\ell=1}^L \text{P}\left(\frac{\sum_{S \in \mathcal{V}^{(\ell)} \setminus \mathcal{X}_3} |S|}{\sum_{S \in \mathcal{R}_{\text{node}}^{(\ell)}} |S|} > \alpha + \epsilon + o(1)\right) \\
&\rightarrow 0
\end{aligned}$$

So statement (2) is proved. The statement (1) can be proved in the similar way. \square

Supplementary Materials for "Distance Assisted Recursive Testing"

S1 Proof of the Lemmas

Proof of Lemma 1. Let $X'_{o,i} = \frac{\mathbf{q}^T \hat{\theta}_i}{\sigma \sqrt{\mathbf{q}^T (\mathbf{W}_i^T \mathbf{W}_i)^{-1} \mathbf{q}}}$, we have $X'_{o,i} \sim N(\eta_i, 1)$ with $\eta_i = \frac{\mathbf{q}^T \theta_i}{\sigma \sqrt{\mathbf{q}^T (\mathbf{W}_i^T \mathbf{W}_i)^{-1} \mathbf{q}}}$. Given $s^2/\sigma^2 \sim \frac{\mathcal{X}^2(n-p_0-1)}{n-p_0-1}$, we have $X_{o,i}/X_i^* = O_p(n^{-1/2})$. Let $[\mathcal{P}_{i0}]^{-1} := \{a \in \mathbb{R} : P(X_{o,i} > a) \geq [m(\log m \log \log m)]^{-1}\}$. Then,

$$\begin{aligned} \sup_{a \in [\mathcal{P}_{i0}]^{-1}} \frac{P(X_i^* > a)}{P(X_{o,i} > a)} &\leq \sup_{a \in [\mathcal{P}_{i0}]^{-1}} \left\{ \frac{P(X_{o,i} > a - \frac{2\sqrt{\log m}}{n^{1/4}})}{P(X_{o,i} > a)} + \frac{P(|s^2/\sigma^2 - 1| > \frac{2\sqrt{\log m}}{n^{1/4}})}{P(X_{o,i} > a)} \right\} \\ &= 1 + o(1) + \sup_{a \in [\mathcal{P}_{i0}]^{-1}} \frac{P(|s^2/\sigma^2 - 1| > \frac{2\sqrt{\log m}}{n^{1/4}})}{P(X_{o,i} > a)} \\ &\leq 1 + o(1) + \frac{P(|s^2/\sigma^2 - 1| > \frac{2\sqrt{\log m}}{n^{1/4}})}{[m(\log m \log \log m)]^{-1}} \end{aligned}$$

Thus, to achieve equation (6), it is sufficient to show

$$P(|s^2/\sigma^2 - 1| > \frac{2\sqrt{\log m}}{n^{1/4}}) = o([m(\log m \log \log m)]^{-1})$$

Let $Y_1, \dots, Y_{n-p_0-1} \stackrel{iid}{\sim} \mathcal{X}^2(1)$ and $Y = \frac{\sum_{k=1}^{n-p_0-1} (Y_k - 1)}{\sqrt{n-p_0-1}}$, we have $Y/\sqrt{n-p_0-1} \sim \frac{\mathcal{X}^2(n-p_0-1)}{n-p_0-1} - 1$.

Thus,

$$\begin{aligned} P(|s^2/\sigma^2 - 1| > \frac{2\sqrt{\log m}}{n^{1/4}}) &= P\left(\left|Y/\sqrt{n-p_0-1}\right| > \frac{2\sqrt{\log m}}{n^{1/4}}\right) \\ &\leq P\left(|Y| > 4\sqrt{\log m}\right) \\ &\stackrel{(a)}{\leq} 2\bar{\Phi}(4\sqrt{\log m})(1 + (1/\log m)^2) \\ &= o([m(\log m \log \log m)]^{-1}) \end{aligned}$$

The inequality (a) is based on Lemma 6.1 in Liu et al. (2013). Thus, the equation (6) holds. \square

Proof of Lemma 2. (1) For $k \in \{1, \dots, c_0\}$, let $q_0 \geq \epsilon(m)$. Also define $b_{1,k}(q_0)$, c_1, \dots, c_k be the value s.t. $P(\sum_{j=1}^k \tilde{X}_j > b_{1,k}(q_0)) = q_0 [\epsilon'(m)]^{\frac{c_0-k}{c_0}}$, and $P(\tilde{X}_1 > c_1) = \dots = P(\tilde{X}_k > c_k) = \epsilon(m) \epsilon'(m)$, respectively. For simplicity sake, we use $b_{1,k}$ to present $b_{1,k}(q_0)$.

Based on the definition, we have

$$b_{1,k} < \sum_{j=1}^k c_j$$

Thus, when $k = 2$,

$$\begin{aligned} & P(\hat{X}_1 + \hat{X}_2 > b_{1,2}) \\ &= P(\hat{X}_1 + \hat{X}_2 > b_{1,2}, \hat{X}_1 > b_{1,2} - c_2, \hat{X}_2 > b_{1,2} - c_1) \\ & \quad + P(\hat{X}_1 + \hat{X}_2 > b_{1,2}, \hat{X}_1 < b_{1,2} - c_2) + P(\hat{X}_1 + \hat{X}_2 > b_{1,2}, \hat{X}_2 < b_{1,2} - c_1) \\ &= P(\hat{X}_1 + \hat{X}_2 > b_{1,2}, c_1 > \hat{X}_1 > b_{1,2} - c_2) + P(\hat{X}_1 > c_1, \hat{X}_2 > b_{1,2} - c_1) \\ & \quad + P(\hat{X}_1 + \hat{X}_2 > b_{1,2}, \hat{X}_1 < b_{1,2} - c_2) + P(\hat{X}_1 + \hat{X}_2 > b_{1,2}, \hat{X}_2 < b_{1,2} - c_1) \end{aligned}$$

Based on construction, the last three terms always smaller than $\epsilon(m) \epsilon'(m)(1 + \delta_4(m))$ for $\delta_4(m) := \max_{i \in \Omega} \sup_{p \in \mathcal{P}'_i} \left| \frac{P(\hat{T}_i < p)}{P(\tilde{T}_i < p)} - 1 \right| \rightarrow 0$, and accordingly, we have

$$\begin{aligned} & P(\hat{X}_1 + \hat{X}_2 > b_{1,2}, c_1 > \hat{X}_1 > b_{1,2} - c_2) + P(\hat{X}_1 > c_1, \hat{X}_2 > b_{1,2} - c_1) \\ & \leq [P(\hat{X}_1 + \tilde{X}_2 > b_{1,2}, c_1 > \hat{X}_1 > b_{1,2} - c_2) + P(\hat{X}_1 > c_1, \tilde{X}_2 > b_{1,2} - c_1)](1 + \delta_4(m)) \\ & \leq [P(\hat{X}_1 + \tilde{X}_2 > b_{1,2}, \hat{X}_1 > b_{1,2} - c_2, \tilde{X}_2 > b_{1,2} - c_1)](1 + \delta_4(m)) \\ & \leq P(\tilde{X}_1 + \tilde{X}_2 > b_{1,2}, \tilde{X}_1 > b_{1,2} - c_2, \tilde{X}_2 > b_{1,2} - c_1)(1 + \delta_4(m))^2 \end{aligned}$$

Based on similar arguments, we can also have

$$\begin{aligned} & P(\hat{X}_1 + \hat{X}_2 > b_{1,2}, c_1 > \hat{X}_1 > b_{1,2} - c_2) + P(\hat{X}_1 > c_1, \hat{X}_2 > b_{1,2} - c_1) \\ & \geq P(\tilde{X}_1 + \tilde{X}_2 > b_{1,2}, \tilde{X}_1 > b_{1,2} - c_2, \tilde{X}_2 > b_{1,2} - c_1)(1 - \delta_4(m))^2 \end{aligned}$$

Thus,

$$\sup_{q_0 \geq \epsilon(m)} \left[\epsilon'(m) \right]^{\frac{c_0-k}{c_0}} \left| \frac{P(\hat{X}_1 + \hat{X}_2 > b_{1,2})}{P(\tilde{X}_1 + \tilde{X}_2 > b_{1,2})} - 1 \right| \rightarrow 0$$

Similarly, if $\sup_{q_0 \geq \epsilon(m)} \left[\epsilon'(m) \right]^{\frac{c_0-k}{c_0}} \left| \frac{P(\sum_{j=1}^k \hat{X}_j > b_{1,k})}{P(\sum_{j=1}^k \tilde{X}_j > b_{1,k})} - 1 \right| \rightarrow 0$, we can have

$$\sup_{q_0 \geq \epsilon(m)} \left[\epsilon'(m) \right]^{\frac{c_0-k}{c_0}} \left| \frac{P(\sum_{j=1}^{k+1} \hat{X}_j > b_{1,k+1})}{P(\sum_{j=1}^{k+1} \tilde{X}_j > b_{1,k+1})} - 1 \right| \rightarrow 0$$

Thus, we can get (1). In addition, based on the similar arguments, we can get (2).

□

Proof of Lemma 3. Let $Z'_1, \dots, Z'_K \stackrel{iid}{\sim} N(0, 1)$, with $2 \leq K < M^{L-1}$. Define the set $\mathfrak{M} = \{\mathcal{M}_1 \subset \{1, \dots, m\} : 1 \leq |\mathcal{M}_1| \leq K-1\}$. In order to show statement (1), it is suffice to show:

$$\lim_{m \rightarrow \infty} \sup_{\mathcal{M}_1 \in \mathfrak{M}} \sup_{\substack{c_1 \in [\beta_0, \gamma] \\ c_2 \in [0, \gamma]}} \frac{P\left(\frac{1}{\sqrt{K}} \sum_{i=1}^K Z'_i > c_2, \frac{1}{\sqrt{|\mathcal{M}_1|}} \sum_{j \in \mathcal{M}_1} Z'_j > c_1\right)}{P\left(\frac{1}{\sqrt{K}} \sum_{i=1}^K Z'_i > c_2\right)} = 0$$

Here, $\beta_0 = b\beta$, with $b = \sqrt{\frac{2M^{L-1}+1-r_1}{2(1-r_1)}} \in \left(\sqrt{\frac{M^{L-1}}{(M^{L-1}+1)(1-r_1)}}, 1\right)$

For simplification, let $k_1 = |\mathcal{M}_1|$. For Z_1 and $Z_2 \stackrel{iid}{\sim} N(0, 1)$, define

$$\mathcal{D}_m = \left\{ c_2 \in (0, \gamma) : \frac{d}{dc_2} \frac{P\left(\sqrt{\frac{k_1}{K}} Z_1 + \sqrt{\frac{K-k_1}{K}} Z_2 > c_2, Z_1 > \beta_0\right)}{P\left(\sqrt{\frac{k_1}{K}} Z_1 + \sqrt{\frac{K-k_1}{K}} Z_2 > c_2\right)} = 0 \right\}$$

, then

$$\begin{aligned}
& \sup_{\substack{c_1 \in [\beta_0, \gamma] \\ c_2 \in [0, \gamma]}} \frac{P\left(\frac{1}{\sqrt{K}} \sum_{i=1}^K Z'_i > c_2, \frac{1}{\sqrt{|\mathcal{M}_1|}} \sum_{j \in \mathcal{M}_1} Z'_j > c_1\right)}{P\left(\frac{1}{\sqrt{K}} \sum_{i=1}^K Z'_i > c_2\right)} \leq 2 \sup_{c_2 \in [0, \gamma]} \frac{P\left(\sqrt{\frac{k_1}{K}} Z_1 + \sqrt{\frac{K-k_1}{K}} Z_2 > c_2, Z_1 > \beta_0\right)}{P\left(\sqrt{\frac{k_1}{K}} Z_1 + \sqrt{\frac{K-k_1}{K}} Z_2 > c_2\right)} \\
& \leq 2 \max \left\{ \sup_{\substack{c_2=0 \text{ or } \gamma}} \frac{P\left(\sqrt{\frac{k_1}{K}} Z_1 + \sqrt{\frac{K-k_1}{K}} Z_2 > c_2, Z_1 > \beta_0\right)}{P\left(\sqrt{\frac{k_1}{K}} Z_1 + \sqrt{\frac{K-k_1}{K}} Z_2 > c_2\right)}, \sup_{c_2 \in \mathcal{D}_m} \frac{P\left(\sqrt{\frac{k_1}{K}} Z_1 + \sqrt{\frac{K-k_1}{K}} Z_2 > c_2, Z_1 > \beta_0\right)}{P\left(\sqrt{\frac{k_1}{K}} Z_1 + \sqrt{\frac{K-k_1}{K}} Z_2 > c_2\right)} \right\}
\end{aligned}$$

(i). When $c_2 = 0$,

$$\begin{aligned}
& \lim_{m \rightarrow \infty} \frac{P\left(\sqrt{\frac{k_1}{K}} Z_1 + \sqrt{\frac{K-k_1}{K}} Z_2 > c_2, Z_1 > \beta_0\right)}{P\left(\sqrt{\frac{k_1}{K}} Z_1 + \sqrt{\frac{K-k_1}{K}} Z_2 > c_2\right)} \\
& = \lim_{m \rightarrow \infty} 2P\left(\sqrt{\frac{k_1}{K}} Z_1 + \sqrt{\frac{K-k_1}{K}} Z_2 > c_2, Z_1 > \beta_0\right) \\
& = 0
\end{aligned}$$

(ii). When $c_2 = \gamma$, $c_2/\beta_0 = \frac{1}{b} \sqrt{\frac{1}{1-r_1}}$,

$$\begin{aligned}
& \lim_{m \rightarrow \infty} \frac{P\left(\sqrt{\frac{k_1}{K}} Z_1 + \sqrt{\frac{K-k_1}{K}} Z_2 > c_2, Z_1 > \beta_0\right)}{P\left(\sqrt{\frac{k_1}{K}} Z_1 + \sqrt{\frac{K-k_1}{K}} Z_2 > c_2\right)} \\
& = \lim_{\beta_0 \rightarrow \infty} \frac{\int_{\beta_0}^{\infty} \int_{S\sqrt{\frac{K}{K-k_1}}\beta_0 - \sqrt{\frac{k_1}{K-k_1}}z_1}^{\infty} \phi(z_1) \phi(z_2) dz_2 dz_1}{\int_{S\beta_0}^{\infty} \phi(z) dz} \\
& \leq C \lim_{\beta_0 \rightarrow \infty} \frac{\int_{S\sqrt{\frac{K}{K-k_1}}\beta_0 - \sqrt{\frac{k_1}{K-k_1}}\beta_0}^{\infty} \phi(\beta_0) \phi(z) dz + \int_{\beta_0}^{\infty} \phi(z) \phi(S\sqrt{\frac{K}{K-k_1}}\beta_0 - \sqrt{\frac{k_1}{K-k_1}}z) dz}{\phi(S\beta_0)} \quad (\text{L'Hopital's rule}) \\
& \leq C \lim_{\beta_0 \rightarrow \infty} \left[\exp \left\{ -\frac{\beta_0^2}{2} \left(S\sqrt{\frac{k_1}{K-k_1}} - \sqrt{\frac{K}{K-k_1}} \right)^2 \right\} \right. \\
& \quad \left. + \int_{\beta_0}^{\infty} \exp \left\{ -\frac{1}{2} \left(\sqrt{\frac{K}{K-k_1}}z - S\sqrt{\frac{k_1}{K-k_1}}\beta_0 \right)^2 \right\} dz \right] \\
& = 0
\end{aligned}$$

Where $S = \frac{1}{b} \sqrt{\frac{1}{1-r_1}}$

(iii). When $c_2 \in \mathcal{D}_m$, given

$$\begin{aligned}
0 &= \frac{d}{dc_2} \frac{P\left(\sqrt{\frac{k_1}{K}}Z_1 + \sqrt{\frac{K-k_1}{K}}Z_2 > c_2, Z_1 > \beta_0\right)}{P\left(\sqrt{\frac{k_1}{K}}Z_1 + \sqrt{\frac{K-k_1}{K}}Z_2 > c_2\right)} \\
&= \frac{1}{P\left(\sqrt{\frac{k_1}{K}}Z_1 + \sqrt{\frac{K-k_1}{K}}Z_2 > c_2\right)^2} \left\{ \right. \\
&\quad P\left(\sqrt{\frac{k_1}{K}}Z_1 + \sqrt{\frac{K-k_1}{K}}Z_2 > c_2\right) \frac{d}{dc_2} P\left(\sqrt{\frac{k_1}{K}}Z_1 + \sqrt{\frac{K-k_1}{K}}Z_2 > c_2, Z_1 > \beta_0\right) \\
&\quad \left. - P\left(\sqrt{\frac{k_1}{K}}Z_1 + \sqrt{\frac{K-k_1}{K}}Z_2 > c_2, Z_1 > \beta_0\right) \frac{d}{dc_2} P\left(\sqrt{\frac{k_1}{K}}Z_1 + \sqrt{\frac{K-k_1}{K}}Z_2 > c_2\right) \right\}
\end{aligned}$$

We have

$$\frac{P\left(\sqrt{\frac{k_1}{K}}Z_1 + \sqrt{\frac{K-k_1}{K}}Z_2 > c_2, Z_1 > \beta_0\right)}{P\left(\sqrt{\frac{k_1}{K}}Z_1 + \sqrt{\frac{K-k_1}{K}}Z_2 > c_2\right)} = \frac{\frac{d}{dc_2} P\left(\sqrt{\frac{k_1}{K}}Z_1 + \sqrt{\frac{K-k_1}{K}}Z_2 > c_2, Z_1 > \beta_0\right)}{\frac{d}{dc_2} P\left(\sqrt{\frac{k_1}{K}}Z_1 + \sqrt{\frac{K-k_1}{K}}Z_2 > c_2\right)}$$

Therefore,

$$\begin{aligned}
&\sup_{c_2 \in \mathcal{D}_m} \frac{P\left(\sqrt{\frac{k_1}{K}}Z_1 + \sqrt{\frac{K-k_1}{K}}Z_2 > c_2, Z_1 > \beta_0\right)}{P\left(\sqrt{\frac{k_1}{K}}Z_1 + \sqrt{\frac{K-k_1}{K}}Z_2 > c_2\right)} \\
&= \sup_{c_2 \in \mathcal{D}_m} \frac{\frac{d}{dc_2} P\left(\sqrt{\frac{k_1}{K}}Z_1 + \sqrt{\frac{K-k_1}{K}}Z_2 > c_2, Z_1 > \beta_0\right)}{\frac{d}{dc_2} P\left(\sqrt{\frac{k_1}{K}}Z_1 + \sqrt{\frac{K-k_1}{K}}Z_2 > c_2\right)} \\
&= \sup_{c_2 \in \mathcal{D}_m} C \int_{\beta_0}^{\infty} \exp \left\{ -\frac{1}{2} \left(\sqrt{\frac{K}{K-k_1}} z - \sqrt{\frac{k_1}{K-k_1}} c_2 \right)^2 \right\} dz \\
&\leq C \int_{\beta_0}^{\infty} \exp \left\{ -\frac{1}{2} \left(\sqrt{\frac{K}{K-k_1}} z - \sqrt{\frac{k_1}{K-k_1}} \gamma \right)^2 \right\} dz \\
&\rightarrow 0
\end{aligned}$$

Combine (i), (ii) and (iii), we have

$$\lim_{m \rightarrow \infty} \sup_{\mathcal{M}_1 \in \mathfrak{M}} \sup_{\substack{c_1 \in [\beta_0, \gamma] \\ c_2 \in [0, \gamma]}} \frac{P\left(\frac{1}{\sqrt{K}} \sum_{i=1}^K Z_i > c_2, \left| \frac{1}{\sqrt{|\mathcal{M}_1|}} \sum_{j \in \mathcal{M}_1} Z_j \right| > c_1\right)}{P\left(\frac{1}{\sqrt{K}} \sum_{i=1}^K Z_i > c_2\right)} = 0$$

□

Proof of Lemma 4. (i) Prove that (1) can leads to (2):

On $\cap_{t=1}^{\ell} \mathcal{X}^{(t)}$,

$$\sum_{S \in \mathcal{B}_0^{(\ell)}} |S| I(T_S < \hat{t}^{(\ell)}) \leq \sum_{S \in \mathcal{B}_0^{(\ell)}} |S| \hat{t}^{(\ell)} + \left\{ \sum_{S \in \mathcal{B}_0^{(\ell)}} |S| \hat{t}^{(\ell)} \right\} \epsilon$$

Combined with

$$\sum_{S \in \mathcal{B}_0^{(\ell)}} |S| \hat{t}^{(\ell)} \leq \alpha \sum_{S \in \mathcal{B}_0^{(\ell)}} |S| \mathbb{I}\{T_S < \hat{t}^{(\ell)}\}$$

and

$$\begin{aligned} \sum_{S \in \mathcal{B}^{(\ell)}} |S| \mathbb{I}\{T_S < \hat{t}^{(\ell)}\} &= \sum_{S \in \mathcal{B}_0^{(\ell)}} |S| \mathbb{I}\{T_S < \hat{t}^{(\ell)}\} + \sum_{S \in \mathcal{B}_1^{(\ell)}} |S| \mathbb{I}\{T_S^{(\ell)} \leq \hat{t}^{(\ell)}\} \\ &\leq \sum_{S \in \mathcal{B}_0^{(\ell)}} |S| \mathbb{I}\{T_S^{(\ell)} < \hat{t}^{(\ell)}\} + Cm^{r_1} \end{aligned}$$

We have:

$$(1 - \alpha - \epsilon) \sum_{S \in \mathcal{B}_0^{(\ell)}} |S| \hat{t}^{(\ell)} \leq \alpha Cm^{r_1}$$

Thus, $2|\mathcal{B}_0^{(\ell)}| \hat{t}^{(\ell)} \leq \sum_{S \in \mathcal{B}_0^{(\ell)}} |S| \hat{t}^{(\ell)} \leq \frac{\alpha}{1-\alpha-\epsilon} m^{r_1}$, for any $1 \leq \ell \leq L$.

When $\ell = 1$, by $|\mathcal{B}_0^{(1)}| = m_0 = m(1 + o(1))$, we have $\hat{t}^{(\ell)} \leq Cm^{(r_1-1)}$.

When $\ell \geq 2$, on $\cap_{k=1}^{\ell} \mathcal{X}^{(k)}$, we have

$$\max_{k=1, \dots, \ell} \{FDP^{(k)} - \alpha\} < \epsilon$$

which leads to $|\mathcal{B}_0^{(\ell)}| / |\mathcal{B}^{(\ell)}| \rightarrow 1$. And accordingly, $\hat{t}^{(\ell)} \leq Cm^{(r_1-1)}$.

(ii) Prove that statement (2) leads to statement (3)

On layer 1, $\bar{\Phi}(\hat{c}_S) = \hat{t}^{(1)} \leq C(m)^{r_1-1}$. On layer $\ell \geq 2$ and $\cap_{h=1}^{\ell} \mathcal{X}^{(h)}$, for all $S \in \mathcal{B}^{(\ell)}$,

$$\bar{\Phi}(\hat{c}_S) \leq G_S(\hat{c}_S) + \sum_{S' \in \mathcal{U}(S)} \bar{\Phi}(\hat{c}_{S'}) \quad (\text{S1})$$

Suppose $\bar{\Phi}(\hat{c}_{S'}) \leq C(m)^{r_1-1}$ for $S' \in \cup_{k=1}^{\ell-1} \mathcal{B}^{(k)}$, then together with $G_S(\hat{c}_S) = \hat{t}^{(\ell)} \leq Cm^{r_1-1}$ and (S1), we have

$$\hat{c}_S \geq \sqrt{2(1-r_1) \log m - \log \log m} = \beta$$

for all $S \in \mathcal{B}^{(\ell)}$.

In addition, for $S \in \mathcal{B}^{(\ell)}$, on $\cap_{h=1}^{\ell-1} \mathcal{X}^{(h)}$,

$$G_S(\hat{c}_S)[1 - \bar{\Phi}(\beta_0)]^{|\mathcal{U}(S)|} \leq \bar{\Phi}(\hat{c}_S) \quad (\text{S2})$$

So we have $\bar{\Phi}(\hat{c}_S) \geq \hat{t}^{(\ell)}(1 + o(1))$, and accordingly, $\hat{c}_S \leq \gamma$.

Note that the $\hat{c}_S \leq \gamma$ only depends on the statement (2) on layer $\ell - 1$. Thus, we can apply the conclusion to show $P(m_0 \hat{t}^{(\ell)} > c \log m) \rightarrow 1$ in the proof of theorem 1.

(iii) Prove that statement (1) holds on layer 1 ($\ell = 1$):

Let $0 = c_0 < \dots < c_{\lceil \gamma(\log m \log \log m)^{1/2} \rceil} = \gamma$ satisfy $c_k - c_{k-1} = \frac{1}{\sqrt{\log m \log \log m}}$ for $1 \leq k < \lceil \gamma(\log m \log \log m)^{1/2} \rceil$ and $c_{\lceil \gamma(\log m \log \log m)^{1/2} \rceil} - c_{\lceil \gamma(\log m \log \log m)^{1/2} \rceil - 1} \leq \frac{1}{\sqrt{\log m \log \log m}}$. We can get the corresponding p-values sequence $q_0 > \dots > q_{\lceil \gamma(\log m \log \log m)^{1/2} \rceil}$ with $q_k = 1 - \Phi(c_k)$. Let value $q^{(1)} = \frac{C^{(1)} \log m}{m}$, by (28), we have $P(\hat{t} > q^{(1)}) \rightarrow 1$. We define the working p-value sequence on layer 1 as $P_{sub}^{(1)} = \{q_0, \dots, q_{k^{(1)}}, q^{(1)}\}$, where $k^{(1)} \in \{0, \dots, \lceil \gamma(\log m \log \log m)^{1/2} \rceil - 1\}$ is the index s.t. $q_{k^{(1)}} \geq q^{(1)}$ and $q_{k^{(1)}+1} \leq q^{(1)}$.

Define

$$\mathcal{B}_{01}^{(1)} = \{\{i\} : i = 1, \dots, m, i \neq \Gamma\}$$

If $\forall \epsilon > 0$,

$$P\left(\max_{q \in P_{sub}^{(1)}} \left| \frac{\sum_{S \in \mathcal{B}_{01}^{(1)}} I(X_S > \bar{\Phi}^{-1}(q)) - \sum_{S \in \mathcal{B}_{01}^{(1)}} P(X_S > \bar{\Phi}^{-1}(q))(1 + \delta_{0m})}{\sum_{S \in \mathcal{B}_{01}^{(1)}} q} \right| > \epsilon \right) \rightarrow 0 \quad (\text{S3})$$

Then,

$$\begin{aligned} & P\left(\max_{q \in P_{sub}^{(1)}} \frac{\sum_{S \in \mathcal{B}_0^{(1)}} I(T_S^{(1)} < q) - \sum_{S \in \mathcal{B}_0^{(1)}} q}{\sum_{S \in \mathcal{B}_0^{(1)}} q} > \epsilon\right) \\ & \leq P\left(\max_{q \in P_{sub}^{(1)}} \frac{\sum_{S \in \mathcal{B}_0^{(1)}} I(X_S > \bar{\Phi}^{-1}(q)) - \sum_{S \in \mathcal{B}_0^{(1)}} P(\tilde{X}_S > \bar{\Phi}^{-1}(q))}{\sum_{S \in \mathcal{B}_0^{(1)}} q} > \epsilon\right) \\ & \leq P\left(\max_{q \in P_{sub}^{(1)}} \frac{\sum_{S \in \mathcal{B}_{01}^{(1)}} I(X_S > \bar{\Phi}^{-1}(q)) - \sum_{S \in \mathcal{B}_{01}^{(1)}} P(X_S > \bar{\Phi}^{-1}(q))(1 + \delta_{0m})}{\sum_{S \in \mathcal{B}_0^{(1)}} q} > \epsilon - o\left(\frac{1}{\log \log m}\right)\right) \\ & \leq P\left(\max_{q \in P_{sub}^{(1)}} \left| \frac{\sum_{S \in \mathcal{B}_{01}^{(1)}} I(X_S > \bar{\Phi}^{-1}(q)) - \sum_{S \in \mathcal{B}_{01}^{(1)}} P(X_S > \bar{\Phi}^{-1}(q))(1 + \delta_{0m})}{\sum_{S \in \mathcal{B}_0^{(1)}} q} \right| > \epsilon - o\left(\frac{1}{\log \log m}\right)\right) \\ & = o(1) \end{aligned} \quad (\text{S4})$$

Together with the fact that $\sup_{j=1, \dots, k} \left| \frac{q_{(j)}^{(1)}}{q_{(j-1)}^{(1)}} - 1 \right| = o(1)$, we have

$$P\left(\sup_{q \in [\frac{1}{m \log m}, \alpha]} \frac{\sum_{S \in \mathcal{B}_0^{(1)}} I(T_S < q) - \sum_{S \in \mathcal{B}_0^{(1)}} q}{\sum_{S \in \mathcal{B}_0^{(1)}} q} > \epsilon\right) = o(1)$$

Thus, to prove (1) holds on layer 1, we only need to show (S3).

Define $C_{sub}^{(1)} = \{c_0, \dots, c_{k'}, c'\}$, with $c' = \bar{\Phi}^{-1}(q')$. In order to show (S3), it is suffice to show

$$\int_0^{c'} P\left\{ \left| \frac{\sum_{S \in \mathcal{B}_{01}^{(1)}} I(X_S > c) - P(X_S > c)(1 + \delta_{0m})}{\sum_{S \in \mathcal{B}_0^{(1)}} \bar{\Phi}(c)} \right| \geq \epsilon \right\} dc = o\left(\frac{1}{\sqrt{\log m \log \log m}}\right) \quad (\text{S5})$$

Note that by Markov inequality,

$$\begin{aligned}
& P\left\{\left|\frac{\sum_{S \in \mathcal{B}_{01}^{(1)}} [I(X_S > c) - P(X_S > c)(1 + \delta_{0m})]}{\sum_{S \in \mathcal{B}_0^{(1)}} \bar{\Phi}(c)}\right| \geq \epsilon\right\} \\
& \leq P\left\{\left|\frac{\sum_{S \in \mathcal{B}_{01}^{(1)}} [I(X_S > c) - P(X_S > c)]}{\sum_{S \in \mathcal{B}_0^{(1)}} \bar{\Phi}(c)}\right| \geq \epsilon - (1 + \delta_{0m})\delta_{0m}\right\} \\
& \leq \frac{E\left(\sum_{S \in \mathcal{B}_{01}^{(1)}} [I(X_S > c) - P(X_S > c)]\right)^2}{\left(\sum_{S \in \mathcal{B}_0^{(1)}} \bar{\Phi}(c)\right)^2 [\epsilon - (1 + \delta_{0m})\delta_{0m}]^2} \\
& \leq \frac{C}{\sum_{S \in \mathcal{B}_{01}^{(1)}} \bar{\Phi}(c)}
\end{aligned}$$

So we can prove (S5).

(iv) Prove that statement (1) holds on layer $\ell \geq 2$ when statement (1) holds on previous layers:

In view of statement (3) and Lemma 3, we have

$$\sup_{k=0, \dots, \lceil \gamma(\log m \log \log m)^{1/2} \rceil} \left| \frac{G_S(c_k)}{\bar{\Phi}(c_k)} - 1 \right| = o(1)$$

Define

$$\mathcal{B}_{01}^{(\ell)} = \{S \in \mathcal{B}_0^{(\ell)} : S \cap \Gamma = \emptyset\}.$$

So similar to (iii), we first define the working p-value sequence on layer ℓ as $P_{sub}^{(\ell)} = \{q_0, \dots, q_{k^{(\ell)}}, q^{(\ell)}\}$, where $q^{(\ell)} = \frac{C^{(\ell)} \log m}{m}$, and $k^{(\ell)} \in \{0, \dots, \lceil \gamma(\log m \log \log m)^{1/2} \rceil - 1\}$ is the index s.t. $q_{k^{(\ell)}} \geq q^{(\ell)}$ and $q_{k^{(\ell)}+1} \leq q^{(\ell)}$. Together with statement (3), Lemma 2 and Lemma 3, there exists $\delta_5(m) \rightarrow 0$

with

$$\begin{aligned}
& \max_{S \in \mathcal{B}_{01}^{(\ell)}} \frac{P(X_S > \bar{\Phi}^{-1}(q) | \mathcal{Q}^{(1:\ell-1)})}{q} \\
& \leq \max_{S \in \mathcal{B}_{01}^{(\ell)}} \frac{P(X_S > \bar{\Phi}^{-1}(q))}{P(Z_S > \bar{\Phi}^{-1}(q)) \prod_{S' \in \mathcal{U}(S)} P(X_{S'} \leq \beta)} \\
& \leq 1 + \delta_5(m)
\end{aligned}$$

Then $\forall \epsilon > 0$, by following the similar arguments in (iii), we can have

$$\begin{aligned}
& P \left(\max_{q \in P_{sub}^{(\ell)}} \left| \frac{\sum_{S \in \mathcal{B}_{01}^{(\ell)}} |S| I(X_S > \bar{\Phi}^{-1}(q)) - \sum_{S \in \mathcal{B}_{01}^{(\ell)}} |S| P(X_S > \bar{\Phi}^{-1}(q) | \mathcal{Q}^{(1:\ell-1)}) (1 + \delta_{0m})}{\sum_{S \in \mathcal{B}_{01}^{(\ell)}} |S| q} \right| > \epsilon \middle| \mathcal{Q}^{(1:\ell-1)} \right) \\
& \rightarrow 0
\end{aligned} \tag{S6}$$

Then,

$$\begin{aligned}
& P \left(\max_{q \in P_{sub}^{(\ell)}} \frac{\sum_{S \in \mathcal{B}_0^{(\ell)}} |S| I(T_S < q) - \sum_{S \in \mathcal{B}_0^{(\ell)}} |S| q}{\sum_{S \in \mathcal{B}_0^{(\ell)}} |S| q} > \epsilon + o(1/\log \log m) \middle| \mathcal{Q}^{(1:\ell-1)} \right) \\
& \leq P \left(\max_{q \in P_{sub}^{(\ell)}} \frac{\sum_{S \in \mathcal{B}_{01}^{(\ell)}} |S| I(X_S > \bar{\Phi}^{-1}(q)) - \sum_{S \in \mathcal{B}_{01}^{(\ell)}} |S| P(X_S > \bar{\Phi}^{-1}(q) | \mathcal{Q}^{(1:\ell-1)})}{\sum_{S \in \mathcal{B}_{01}^{(\ell)}} |S| q} > \epsilon \middle| \mathcal{Q}^{(1:\ell-1)} \right) \\
& = o(1)
\end{aligned} \tag{S7}$$

Together with the fact that $\sup_{j=1, \dots, k} \left| \frac{q_{(j)}}{q_{(j-1)}} - 1 \right| = o(1)$, we have

$$P \left(\sup_{q \in [\frac{1}{m \log m}, \alpha]} \frac{\sum_{S \in \mathcal{B}_0^{(\ell)}} |S| I(T_S < q) - \sum_{S \in \mathcal{B}_0^{(\ell)}} |S| q}{\sum_{S \in \mathcal{B}_0^{(\ell)}} |S| q} > \epsilon \middle| \mathcal{Q}^{(1:\ell-1)} \right) = o(1)$$

□

Proof of Lemma 5. When $\ell = 1$:

for $\delta = 1/m^4$,

$$\begin{aligned}
\sum_{S \in \mathcal{B}_0^{(1)}} |S| \hat{t}^{(1)} &\leq \alpha \sum_{S \in \mathcal{B}^{(1)}} |S| I(T_S < \hat{t}^{(1)}) \\
&\leq \alpha \sum_{S \in \mathcal{B}^{(1)}} |S| I(T_S < \hat{t}^{(1)} + \delta) \\
&\leq \sum_{S \in \mathcal{B}_0^{(1)}} |S| \hat{t}^{(1)} (1 + o(1))
\end{aligned} \tag{S8}$$

Assume (22) holds on layer $1, \dots, \ell - 1$. Then,

$$\sum_{S \in \mathcal{B}_0^{(\ell)}} |S| \hat{t}^{(\ell)} \leq \alpha(1 + o(1)) \sum_{S \in \mathcal{B}^{(\ell)}} |S| I(T_S < \hat{t}^{(\ell)})$$

Thus, by following the similar arguments on (S8), we can get (22) on layer ℓ . \square

S2 Additional numerical results for assessing impact of the parameter M

In this section, we numerically investigate the impact of the choice of M by comparing the numerical results when $M = 3$ and $M = \infty$. When $M = 3$, the tuning parameters are same to the parameters in A. When $M = \infty$, in order to have a relatively fair comparison, we set the same total layer L as the value in A. The selection procedure of $g^{(\ell)}$ is similar to A. Based on the Algorithm 3, we have

- If $(n, m) = (90, 100)$: we set $g^{(2)} = \frac{16}{\sqrt{n \log m \log \log m}}$
- If $(n, m) = (300, 1000)$: we set $g^{(2)} = \frac{12}{\sqrt{n \log m \log \log m}}$, $g^{(3)} = \frac{26}{\sqrt{n \log m \log \log m}}$ and $g^{(4)} = \frac{44}{\sqrt{n \log m \log \log m}}$.

Figure S1 compares the performance between two different M values under SE1-SE5. We

only compare the performance on the top layer of the aggregation tree. Based on the figure, our method is still valid with FDR control when $M = \infty$.

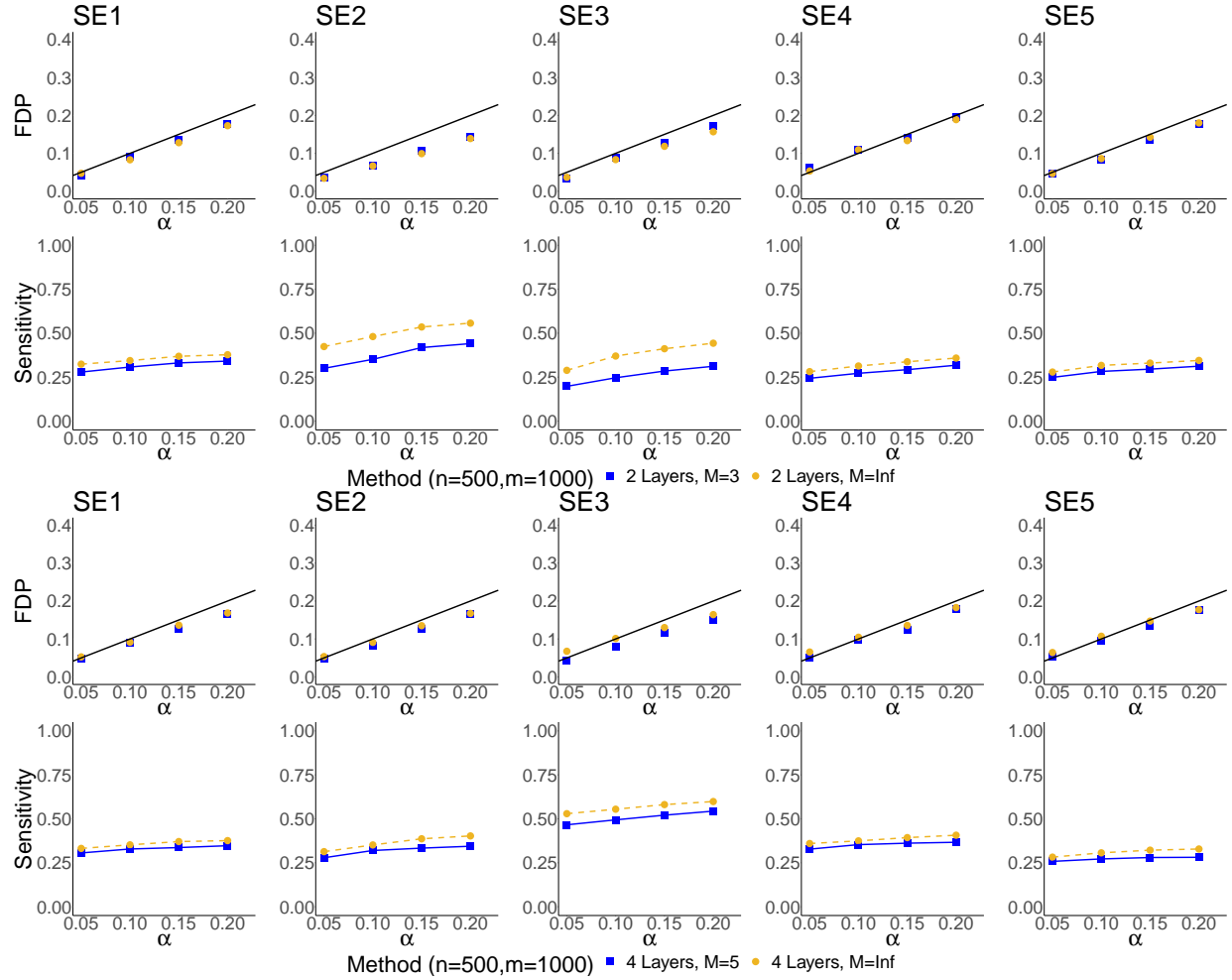


Figure S1: Additional simulation results for setting SE1-SE5. The first two rows represent the results in the setting $(n, m) = (90, 100)$, and the second two rows represent the results in the setting $(n, m) = (300, 1000)$.

Table S1: The number of non-single-child nodes based on value $g \in G^{(\ell)}$ when $M = \infty$. For simplicity purpose, the value g is represented by its nominator: $g' = g \times \sqrt{n \log m \log \log m}$. The selected g' and its corresponding $|\tilde{\mathcal{A}}^{(\ell)}(g)|$ is highlighted in bold.

(1) $(n, m) = (90, 100)$:

Layer 2	g'	2	4	6	8	10	12	14	16	18	20	22	24	...
	$ \tilde{\mathcal{A}}^{(2)}(g) $	5	10	17	22	29	30	30	35	32	31	29	28	...

(2) $(n, m) = (300, 1000)$:

Layer 2	g'	2	4	6	8	10	12	14	16	18	20	...			
	$ \tilde{\mathcal{A}}^{(2)}(g) $	49	149	239	291	300	303	295	288	263	245	...			
Layer 3	g'	14	16	18	20	22	24	26	28	30	32	34	...		
	$ \tilde{\mathcal{A}}^{(3)}(g) $	53	101	130	148	163	167	169	166	159	152	144	...		
Layer 4	g'	28	30	32	34	36	38	40	42	44	46	48	50	52	...
	$ \tilde{\mathcal{A}}^{(4)}(g) $	17	33	47	56	66	70	74	76	80	79	79	79	77	...

References

Aitchison, J., 1982. The statistical analysis of compositional data. *Journal of the Royal Statistical Society: Series B (Methodological)* 44, 139–160.

Benjamini, Y., Hochberg, Y., 1995. Controlling the false discovery rate: a practical and powerful approach to multiple testing. *Journal of the Royal statistical society: series B (Methodological)* 57, 289–300.

Cai, T.T., Sun, W., Xia, Y., 2020. Laws: A locally adaptive weighting and screening approach to spatial multiple testing. *Journal of the American Statistical Association* , 1–30.

Callahan, B.J., McMurdie, P.J., Rosen, M.J., Han, A.W., Johnson, A.J.A., Holmes, S.P., 2016. Dada2: high-resolution sample inference from illumina amplicon data. *Nature methods* 13, 581.

Claesson, M.J., Jeffery, I.B., Conde, S., Power, S.E., O'connor, E.M., Cusack, S., Harris, H.M., Coakley, M., Lakshminarayanan, B., O'Sullivan, O., et al., 2012. Gut microbiota composition correlates with diet and health in the elderly. *Nature* 488, 178–184.

Dmitrienko, A., Tamhane, A.C., 2013. General theory of mixture procedures for gatekeeping. *Biom J* 55, 402–19. doi:10.1002/bimj.201100258.

Dmitrienko, A., Wiens, B.L., Tamhane, A.C., Wang, X., 2007. Tree-structured gatekeeping tests in clinical trials with hierarchically ordered multiple objectives. *Stat Med* 26, 2465–78. doi:10.1002/sim.2716.

Goeman, J.J., Finos, L., 2012. The inheritance procedure: multiple testing of tree-structured hypotheses. *Stat Appl Genet Mol Biol* 11, Article 11. doi:10.1515/1544-6115.1554.

Goeman, J.J., Mansmann, U., 2008. Multiple testing on the directed acyclic graph of gene ontology. *Bioinformatics* 24, 537–44. doi:10.1093/bioinformatics/btm628.

Guo, W., Lynch, G., Romano, J.P., 2018. A new approach for large scale multiple testing with application to fdr control for graphically structured hypotheses URL: <https://arxiv.org/pdf/1812.00258.pdf>, arXiv:1812.00258.

Jenq, R.R., Ubeda, C., Taur, Y., Menezes, C.C., Khanin, R., Dudakov, J.A., Liu, C., West, M.L., Singer, N.V., Equinda, M.J., et al., 2012. Regulation of intestinal inflammation by microbiota following allogeneic bone marrow transplantation. *Journal of Experimental Medicine* 209, 903–911.

Jukes, T.H., Cantor, C.R., et al., 1969. Evolution of protein molecules. *Mammalian protein metabolism* 3, 21–132.

Kurtz, Z.D., Müller, C.L., Miraldi, E.R., Littman, D.R., Blaser, M.J., Bonneau, R.A., 2015. Sparse and compositionally robust inference of microbial ecological networks. *PLoS computational biology* 11.

Lee, D., Lee, Y., 2016. Extended likelihood approach to multiple testing with directional error control under a hidden markov random field model. *Journal of Multivariate Analysis* 151, 1 – 13. URL: <http://www.sciencedirect.com/science/article/pii/S0047259X16300458>, doi:<https://doi.org/10.1016/j.jmva.2016.07.001>.

Li, Y., Hu, Y.J., Satten, G.A., 2020. A bottom-up approach to testing hypotheses that have a branching tree dependence structure, with error rate control. *Journal of the American Statistical Association* , 1–18URL: <https://doi.org/10.1080%2F01621459.2020.1799811>, doi:[10.1080/01621459.2020.1799811](https://doi.org/10.1080/01621459.2020.1799811).

Liu, J., Peissig, P., Zhang, C., Burnside, E., McCarty, C., Page, D., 2012. Graphical-model based multiple testing under dependence, with applications to genome-wide association studies. *Uncertain Artif Intell* 2012, 511–522.

Liu, W., et al., 2013. Gaussian graphical model estimation with false discovery rate control. *The Annals of Statistics* 41, 2948–2978.

Meijer, R.J., Goeman, J.J., 2015. A multiple testing method for hypotheses structured in a directed acyclic graph. *Biom J* 57, 123–43. doi:10.1002/bimj.201300253.

Schliep, K., 2011. phangorn: phylogenetic analysis in r. *Bioinformatics* 27, 592–593. URL: <https://doi.org/10.1093/bioinformatics/btq706>.

Shu, H., Nan, B., Koepp, R., 2015. Multiple testing for neuroimaging via hidden markov random field. *Biometrics* 71, 741–750.

Soriano, J., Ma, L., 2017. Probabilistic multi-resolution scanning for two-sample differences. *Journal of The Royal Statistical Society Series B-statistical Methodology* 79, 547–572.

Sun, W., Cai, T., 2009. Large-scale multiple testing under dependence. *Journal of the Royal Statistical Society: Series B (Statistical Methodology)* 71, 393–424.

Xie, J., Li, R., 2018. False discovery rate control for high dimensional networks of quantile associations conditioning on covariates. *J R Stat Soc Series B Stat Methodol* 80, 1015–1034. doi:10.1111/rssb.12288.

Yekutieli, D., 2008. Hierarchical false discovery rate-controlling methodology. *Journal of the American Statistical Association* 103, 309–316. URL: <http://www.jstor.org/stable/27640041>.

Zhang, C., Fan, J., Yu, T., 2011. Multiple testing via FDR_L for large scale imaging data. *Annals of statistics* 39, 613.